

# Combined Explanations of the $b \rightarrow s\mu^+\mu^-$ and $b \rightarrow c\tau^-\bar{\nu}$ Anomalies: a General Model Analysis

Jacky Kumar\*

*Department of Physics, Indian Institute of Science Education and Research,  
Mohali, Punjab, 140036 India*

David London† and Ryoutaro Watanabe‡

*Physique des Particules, Université de Montréal,  
C.P. 6128, succ. centre-ville, Montréal, QC, Canada H3C 3J7*

There are four models of tree-level new physics (NP) that can potentially simultaneously explain the  $b \rightarrow s\mu^+\mu^-$  and  $b \rightarrow c\tau^-\bar{\nu}$  anomalies. They are the  $S_3$ ,  $U_3$  and  $U_1$  leptoquarks (LQs), and a triplet of standard-model-like vector bosons ( $VB$ s). Under the theoretical assumption that the NP couples predominantly to the third generation, previous analyses found that, when constraints from other processes are taken into account, the  $S_3$ ,  $U_3$  and  $VB$  models cannot explain the  $B$  anomalies, but  $U_1$  is viable. In this paper, we reanalyze these models, but without any assumption about their couplings. We find that, even in this most general case,  $S_3$  and  $U_3$  are excluded. For the  $U_1$  model, constraints from the semileptonic lepton-flavour-violating (LFV) processes  $B \rightarrow K^{(*)}\mu^\pm\tau^\mp$ ,  $\tau \rightarrow \mu\phi$  and  $\Upsilon \rightarrow \mu\tau$ , which have been largely ignored previously, are found to be very important. Because of the LFV constraints, the pattern of couplings of the  $U_1$  LQ is similar to that obtained with the above theoretical assumption. Also, the LFV constraints render unimportant those constraints obtained using the renormalization group equations. As for the  $VB$  model, it is excluded if the above theoretical assumption is made due to the additional constraints from  $B_s^0$ - $\bar{B}_s^0$  mixing,  $\tau \rightarrow 3\mu$  and  $\tau \rightarrow \mu\nu\bar{\nu}$ . By contrast, we find a different set of NP couplings that both explains the  $b \rightarrow s\mu^+\mu^-$  anomaly and is compatible with all constraints. However, it does not reproduce the measured values of the  $b \rightarrow c\tau^-\bar{\nu}$  anomalies – it would be viable only if future measurements find that the central values of these anomalies are reduced. Even so, this  $VB$  model is excluded by the LHC bounds on high-mass resonant dimuon pairs. This conclusion is reached without any assumptions about the NP couplings.

## I. INTRODUCTION

At the present time, there are a number of measurements of  $B$  decays that are in disagreement with the predictions of the standard model (SM). These can be separated into two categories:

1.  $b \rightarrow s\mu^+\mu^-$ : discrepancies with the SM can be found in several observables in  $B \rightarrow K^*\mu^+\mu^-$  [1–5] and  $B_s^0 \rightarrow \phi\mu^+\mu^-$  [6, 7] decays, as well as in the observation of lepton flavour universality (LFU) violation in  $R_K \equiv \mathcal{B}(B^+ \rightarrow K^+\mu^+\mu^-)/\mathcal{B}(B^+ \rightarrow K^+e^+e^-)$  [8] and  $R_{K^*} \equiv \mathcal{B}(B^0 \rightarrow K^{*0}\mu^+\mu^-)/\mathcal{B}(B^0 \rightarrow K^{*0}e^+e^-)$  [9]. Following the announcement of the  $R_{K^*}$  result, several papers performed a combined analysis of the various  $b \rightarrow s\ell^+\ell^-$  observables [10–17]. The general consensus was that the discrepancy with the SM is at the level of  $4\text{--}6\sigma$  (the range reflects the fact that the groups used different ways of treating the theoretical hadronic uncertainties). Apart from the size of the disagreement, what is particularly intriguing here is that the data can all be explained if there is new physics (NP) in  $b \rightarrow s\mu^+\mu^-$  transitions.
2.  $b \rightarrow c\tau^-\bar{\nu}$ : there are also measurements of LFU violation in  $R_{D^{(*)}} \equiv \mathcal{B}(\bar{B} \rightarrow D^{(*)}\tau^-\bar{\nu}_\tau)/\mathcal{B}(\bar{B} \rightarrow D^{(*)}\ell^-\bar{\nu}_\ell)$  ( $\ell = e, \mu$ ) [18–21] and  $R_{J/\psi} \equiv \mathcal{B}(B_c^+ \rightarrow J/\psi\tau^+\nu_\tau)/\mathcal{B}(B_c^+ \rightarrow J/\psi\mu^+\nu_\mu)$  [22]. Following the measurements of  $R_{D^{(*)}}$ , updated studies of the SM predictions were performed [23, 24]. It was found that, together, the deviation of the  $R_D$  and  $R_{D^*}$  measurements from the SM predictions is at the  $4\sigma$  level. The discrepancy in  $R_{J/\psi}$  is  $1.7\sigma$  [25]. These suggest the presence of NP in  $b \rightarrow c\tau^-\bar{\nu}$  decays.

Much work was done examining NP models that could explain the  $b \rightarrow s\mu^+\mu^-$  or  $b \rightarrow c\tau^-\bar{\nu}$  anomalies. One conclusion of these studies was that the discrepancies can be explained by NP that couples principally to left-handed (LH) particles, i.e., its interactions are of the form  $(V - A) \times (V - A)$ . In Ref. [26], it was pointed out that, if the

\* jkumar@iisermohali.ac.in

† london@lps.umontreal.ca

‡ watanabe@lps.umontreal.ca

NP couples to LH particles, one can relate the neutral-current  $b \rightarrow s\mu^+\mu^-$  and charged-current  $b \rightarrow c\tau^-\bar{\nu}$  transitions using the SM  $SU(2)_L$  symmetry. That is, it is possible to find a NP model that can simultaneously explain the  $b \rightarrow s\mu^+\mu^-$  and  $b \rightarrow c\tau^-\bar{\nu}$  anomalies.

Following this observation, there was a great deal of activity examining various aspects of simultaneous explanations of both  $B$ -decay anomalies [27–62]. Many of these papers studied specific models. It was found that, if one insists on LH NP that contributes to both  $b \rightarrow s\mu^+\mu^-$  and  $b \rightarrow c\tau^-\bar{\nu}$  at tree level, there are only four types of NP models. There are three leptoquark (LQ) models: (i)  $S_3$ , containing an  $SU(2)_L$ -triplet scalar LQ, (ii)  $U_3$ , an  $SU(2)_L$ -triplet vector LQ, and (iii)  $U_1$ , an  $SU(2)_L$ -singlet vector LQ. And there is the  $VB$  model, which contains SM-like LH  $W'$  and  $Z'$  vector bosons.

In Refs. [39] and [50], all four models were studied, taking into account not only the  $b \rightarrow s\mu^+\mu^-$  and  $b \rightarrow c\tau^-\bar{\nu}$  data, but also constraints from other processes to which the particular NP contributes. Of the two anomalies, the NP effect in  $b \rightarrow c\tau^-\bar{\nu}$  is larger (in absolute size, not relative to the SM), simply because the process is tree level in the SM. Of the four particles involved in this transition, three of them belong to the third generation, with the fourth in the second generation. It is then quite natural to assume that the NP couples predominantly to the third generation, with the couplings involving the second generation subdominant.

This is the assumption made in Refs. [39] and [50], though its implementation differs in the two papers. In Ref. [39], it is assumed that the NP couples only to the third generation in the weak basis. The couplings to the second generation are induced when one transforms to the mass basis. Since the mixing angles involved in this transformation are small, the couplings in the mass basis obey a hierarchy  $|c_{22}| < |c_{23}|, |c_{32}| < |c_{33}|$ , where the indices indicate the generations. In Ref. [50], an  $U(2)_q \times U(2)_\ell$  flavour symmetry is imposed, so that the NP couples only to the third generation (in the mass basis). The couplings to the second generation are generated by symmetry-breaking terms due to spurions. Here too, the couplings obey the above hierarchy.

We note in passing that the assumption of NP coupling only to the third generation in the weak basis was quite popular. It was applied in a number of papers, on a variety of subjects – model-independent analyses, specific models, and UV completions of the  $VB$  and  $U_1$  models.

In both analyses the  $S_3$ ,  $U_3$  and  $VB$  models were ruled out; only the  $U_1$  model was a viable candidate for explaining all the  $B$ -decay anomalies. But this raises the question: to what extent do these conclusions depend on the assumption regarding the NP couplings? While the idea of NP coupling principally to the third generation is attractive theoretically, it is not the only possibility. If one relaxes this assumption, so that the couplings involving the second generation are no longer subdominant, could we find  $S_3$ ,  $U_3$  or  $VB$  models that can account for the  $b \rightarrow s\mu^+\mu^-$  and  $b \rightarrow c\tau^-\bar{\nu}$  data? How does the  $U_1$  model change in this case?

This is the issue we address in this paper. We focus separately on the LQ and  $VB$  models. In both cases, we work solely in the mass basis. For simplicity, we assume that the NP couplings involving the first generation leptons and down-type quarks are negligible. (This allows us to focus on the second and third generations, which participate in  $b \rightarrow s\mu^+\mu^-$  and  $b \rightarrow c\tau^-\bar{\nu}$ .) Our idea is simply to establish what sizes of NP couplings are required by the data.

We show that the  $S_3$  and  $U_3$  LQ models cannot explain the  $B$ -decay anomalies, even if only constraints from the anomalies and  $B \rightarrow K^{(*)}\nu\bar{\nu}$  are taken into account. On the other hand, the  $U_1$  model is a viable explanation. If only these constraints are imposed, the couplings can take a great many values. However, when one includes the constraints from semileptonic processes that exhibit lepton flavour violation (LFV), namely  $B \rightarrow K^{(*)}\mu^\pm\tau^\mp$ ,  $\tau \rightarrow \mu\phi$  and  $\Upsilon \rightarrow \mu\tau$ , one finds that the region of allowed couplings is greatly reduced. It is similar (though somewhat larger) to that found when the NP couples predominantly to the third generation. In other words, the data actually point in this direction; no theoretical assumptions are necessary.

When one evolves the full Lagrangian from the NP scale down to low energies using the one-loop renormalization group equations (RGEs), one generates new contributions to a variety of operators. It has been argued [35, 47] that the additional constraints due to these new effects lead to an important reduction in the allowed space of couplings. In this paper, we point out that these RGE constraints are not rigorous. More importantly, we show that, if the absolute value of all couplings is taken to be  $\leq 1$ , so that they remain perturbative, the LFV constraints are much more stringent than the RGE constraints.

In the case of the  $VB$  model, the result is different. In this model, there are also tree-level contributions to  $B_s^0$ - $\bar{B}_s^0$  mixing,  $\tau \rightarrow 3\mu$ ,  $\tau \rightarrow \mu\nu\bar{\nu}$  and  $D^0$ - $\bar{D}^0$  mixing, and these lead to additional severe constraints on the couplings. In particular, the  $Z'\mu^\pm\tau^\mp$  coupling must be very small. But if the NP couples principally to the third generation, this coupling is always rather sizeable, so that this  $VB$  model is ruled out.

On the other hand, in this more general case, we find a set of couplings that both explains the  $b \rightarrow s\mu^+\mu^-$  anomaly and is compatible with all constraints. However, it does not reproduce the measured values of the  $b \rightarrow c\tau^-\bar{\nu}$  anomalies. There is an enhancement of  $R_{D^{(*)}}$ , but it is smaller than what is observed. If future measurements of  $R_{D^{(*)}}$  confirm the present measurements, then the  $VB$  model will be ruled out. Still, if it is found that the central values of  $R_{D^{(*)}}$  are reduced, the  $VB$  model could be an explanation of both anomalies. For this reason, as far as the anomalies are concerned, we refer to the model as semi-viable.

Unfortunately, with this set of couplings, the predicted rate for the production of high-mass resonant dimuon pairs at the LHC is larger than the limits placed by ATLAS and CMS. We note that this constraint can be evaded by adding additional, invisible decays of the  $Z'$ . If this possibility is not realized, we find that, in the end, the  $VB$  model is excluded. However, we stress that this is not the result of any assumption about the NP couplings. Rather, it is found simply by taking into account all the flavour constraints and the bound from the LHC dimuon search.

We begin in Sec. II with a summary of the observables necessary for this study. In Sec. III, we examine the leptoquark models. We show that the  $S_3$  and  $U_3$  models are ruled out, determine the pattern of couplings necessary for the  $U_1$  model to explain the  $B$  anomalies, and tabulate the predictions of this model for other processes. A similar study of the  $VB$  model is carried out in Sec. IV. We show that the model is excluded if the  $Z'\mu^\pm\tau^\mp$  coupling is sizeable. We also demonstrate that, if this coupling is very small, the model is semi-viable but also leads to a disagreement with the LHC bounds on the production of high-mass resonant dimuon pairs. We conclude in Sec. V.

## II. OBSERVABLES

The  $B$  anomalies involve the decays  $b \rightarrow s\mu^+\mu^-$  and  $b \rightarrow c\tau^-\bar{\nu}$ , both semileptonic processes with two quarks and two leptons ( $2q2\ell$ ). There are two  $2q2\ell$  operators that are invariant under the full  $SU(3)_C \times SU(2)_L \times U(1)_Y$  gauge group. In the mass basis, they are given by<sup>1</sup>

$$\mathcal{L}_{\text{NP}} = \frac{G_1^{ijkl}}{\Lambda_{\text{NP}}^2} (\bar{Q}_{iL}\gamma_\mu Q_{jL})(\bar{L}_{kL}\gamma^\mu L_{lL}) + \frac{G_3^{ijkl}}{\Lambda_{\text{NP}}^2} (\bar{Q}_{iL}\gamma_\mu \sigma^I Q_{jL})(\bar{L}_{kL}\gamma^\mu \sigma^I L_{lL}) , \quad (1)$$

where  $\sigma^I$  ( $I = 1, 2, 3$ ) are the Pauli matrices, and  $Q_L$  and  $L_L$  are left-handed quark and lepton doublets, defined as

$$Q_L = \begin{pmatrix} V^\dagger u_L \\ d_L \end{pmatrix} , \quad L_L = \begin{pmatrix} \nu_L \\ \ell_L \end{pmatrix} . \quad (2)$$

Here  $V$  denotes the Cabibbo-Kobayashi-Maskawa (CKM) matrix. NP models that simultaneously explain the two  $B$  anomalies are distinguished by their  $G_1$  and  $G_3$  factors.

NP models that can explain the  $b \rightarrow s\mu^+\mu^-$  and  $b \rightarrow c\tau^-\bar{\nu}$  anomalies must contribute to these decays. From the above, we see that they can potentially contribute to other  $2q2\ell$  processes. A complete analysis of any possible NP model must therefore consider constraints from all  $2q2\ell$  observables.

These observables can be separated into neutral-current (NC) and charged-current (CC) processes. The NC observables can themselves be separated into four types: lepton-flavour-conserving (LFC) branching ratios (BRs), lepton-flavour-universality-violating (LFUV) ratios of BRs, lepton-flavour-violating (LFV) decays, and invisible decays. The full list of these observables that have been measured is [65]

$$\begin{aligned} \text{LFC BRs : } & \Upsilon(nS) \rightarrow \ell^+\ell^-; J/\psi \rightarrow \mu^+\mu^-; \phi \rightarrow \mu^+\mu^-; B_s^0 \rightarrow \mu^+\mu^-; B_s^0 \rightarrow \phi\mu^+\mu^-; B \rightarrow K^{(*)}\mu^+\mu^- , \\ \text{LFUV ratios : } & R_{\Upsilon(nS)}^{\ell/\ell'}; R_{J/\psi}^{\mu/e}; R_\phi^{\mu/e}; R_{B \rightarrow K^{(*)}}^{e/\mu} , \\ \text{LFV decays : } & \Upsilon(nS) \rightarrow \mu^\pm\tau^\mp; J/\psi \rightarrow \mu^\pm\tau^\mp; \tau \rightarrow \mu\phi; B \rightarrow K^{(*)}\mu^\pm\tau^\mp , \\ \text{Invisible : } & \Upsilon(nS) \rightarrow \nu\bar{\nu}; J/\psi \rightarrow \nu\bar{\nu}; \phi \rightarrow \nu\bar{\nu}; B_s^0 \rightarrow \phi\nu\bar{\nu}; B \rightarrow K^{(*)}\nu\bar{\nu} . \end{aligned} \quad (3)$$

In the LFC BRs,  $\ell = \tau, \mu$ , while in the LFUV ratios,  $\ell/\ell' = \tau/\mu, \tau/e, \mu/e$ . The CC observables come in two types: LFC BRs and LFUV ratios. These are

$$\begin{aligned} \text{LFC BRs : } & B_c^+ \rightarrow J/\psi\ell^+\nu_\ell; \bar{B} \rightarrow D^{(*)}\ell^-\bar{\nu}_\ell; D_s^+ \rightarrow \ell^+\nu_\ell; \\ & D^+ \rightarrow \bar{K}^0\mu^+\nu_\mu, D^0 \rightarrow K^{(*)-}\mu^+\nu_\mu , \\ \text{LFUV ratios : } & R_{J/\psi}^{\tau/\mu}; R_{D^{(*)}}^{\tau/\ell}; R_{D^{(*)}}^{\mu/e}; R_{D_s}^{\tau/\mu}; R_{D^+ \rightarrow \bar{K}^0}^{\mu/e}, R_{D^0 \rightarrow \bar{K}^{(*)+}}^{\mu/e} . \end{aligned} \quad (4)$$

In the LFC BRs,  $\ell = \tau, \mu$ . In the above,  $R_{\Upsilon(nS)}^{\tau/\mu} \equiv \mathcal{B}(\Upsilon(nS) \rightarrow \tau^+\tau^-)/\mathcal{B}(\Upsilon(nS) \rightarrow \mu^+\mu^-)$ . The other LFUV ratios are defined similarly. There are additional  $2q2\ell$  observables, such as  $\mathcal{B}(B \rightarrow K^*\tau^+\tau^-)$ , LFUV in  $B^- \rightarrow \ell^-\nu_\ell$ , etc., that have not yet been measured, but are likely to be in the near future. These will be included in our discussion of predictions (Sec. III.3).

<sup>1</sup> These operators are also used in the SM Effective Field Theory, see, for example, Refs. [63, 64].

Ideally, analyses of NP models would include constraints from all of these observables. However, most analyses focus only on a subset of these observables, which we call the “minimal constraints.” These include observables that involve the decays  $b \rightarrow s\mu^+\mu^-$  ( $B \rightarrow K^{(*)}\mu^+\mu^-$ ,  $B_s^0 \rightarrow \phi\mu^+\mu^-$ ,  $B_s^0 \rightarrow \mu^+\mu^-$ ,  $R_{K^{(*)}}$ ),  $b \rightarrow c\tau^-\bar{\nu}$  ( $R_{D^{(*)}}$ ,  $R_{J/\psi}$ ) and  $b \rightarrow s\nu\bar{\nu}$  ( $B \rightarrow K^{(*)}\nu\bar{\nu}$ ,  $B_s^0 \rightarrow \phi\nu\bar{\nu}$ ). The effective Hamiltonians for these processes are

$$\begin{aligned} H_{\text{eff}}(b \rightarrow s\mu^+\mu^-) &= -\frac{\alpha G_F}{\sqrt{2}\pi} V_{tb} V_{ts}^* [C_9^{\mu\mu} (\bar{s}_L \gamma^\mu b_L) (\bar{\mu} \gamma_\mu \mu) + C_{10}^{\mu\mu} (\bar{s}_L \gamma^\mu b_L) (\bar{\mu} \gamma_\mu \gamma^5 \mu)] , \\ H_{\text{eff}}(b \rightarrow c\ell_i \bar{\nu}_j) &= \frac{4G_F}{\sqrt{2}} V_{cb} C_V^{ij} (\bar{c}_L \gamma^\mu b_L) (\bar{\ell}_i \gamma_\mu \nu_{jL}) , \\ H_{\text{eff}}(b \rightarrow s\nu_i \bar{\nu}_j) &= -\frac{\alpha G_F}{\sqrt{2}\pi} V_{tb} V_{ts}^* C_L^{ij} (\bar{s}_L \gamma^\mu b_L) (\bar{\nu}_i \gamma_\mu (1 - \gamma^5) \nu_j) , \end{aligned} \quad (5)$$

where the Wilson coefficients include both the SM and NP contributions:  $C_X = C_X(\text{SM}) + C_X(\text{NP})$ . These NP contributions are given by

$$\begin{aligned} C_9^{\mu\mu}(\text{NP}) &= -C_{10}^{\mu\mu}(\text{NP}) = \frac{\pi}{\sqrt{2}\alpha G_F V_{tb} V_{ts}^*} \frac{(G_1 + G_3)^{bs\mu\mu}}{M_{\text{NP}}^2} , \\ C_V^{ij}(\text{NP}) &= -\frac{1}{2\sqrt{2}G_F V_{cb}} \frac{2(VG_3)^{bcij}}{M_{\text{NP}}^2} , \\ C_L^{ij}(\text{NP}) &= \frac{\pi}{\sqrt{2}\alpha G_F V_{tb} V_{ts}^*} \frac{(G_1 - G_3)^{bsij}}{M_{\text{NP}}^2} . \end{aligned} \quad (6)$$

Consider now the other observables. For all  $2q2\ell$  processes, the NP contributes at tree level. This contribution can be significant if the SM contribution to the process is suppressed. This is the case for  $b \rightarrow s\mu^+\mu^-$  (loop level in the SM) and  $b \rightarrow c\tau^-\bar{\nu}$  (the SM amplitude involves the CKM matrix element  $V_{cb} \simeq 0.04$ ). However, if the SM contribution is unsuppressed, then it dominates the NP contribution. This occurs in all NC observables in which there is neither quark nor lepton flavour violation, namely the decays of  $\Upsilon(nS)$ ,  $J/\psi$  and  $\phi$  to  $l^+l^-$  or  $\nu\bar{\nu}$ . It also applies to CC observables governed by the transition  $c \rightarrow s\nu$  ( $D_s^+ \rightarrow l^+\nu_l$ ,  $D^+ \rightarrow \bar{K}^0 l^+\nu_l$ ,  $D^0 \rightarrow K^{(*)-} l^+\nu_l$ ), for which  $V_{cs} \simeq 1$ . For all of these observables, their constraints on the LQ couplings are extremely weak and need not be taken into account.

This leaves only the four LFV observables that can put important constraints on the NP models:

- $B \rightarrow K^{(*)}\mu^\pm\tau^\mp$ : for the final state  $\mu^-\tau^+$  we have

$$C_9^{bs\mu\tau}(\text{NP}) = -C_{10}^{bs\mu\tau}(\text{NP}) = -\frac{\pi}{\sqrt{2}\alpha G_F V_{tb} V_{ts}^*} \frac{(G_1 + G_3)^{bs\mu\tau}}{M_{\text{NP}}^2} .$$

For the final state  $\tau^-\mu^+$  the NP Wilson coefficient  $C_9^{b\tau\mu}(\text{NP}) = -C_{10}^{b\tau\mu}(\text{NP})$  is found by replacing  $bs\mu\tau \rightarrow b\tau\mu$ . The branching ratios for  $B \rightarrow K^{(*)}\mu^-\tau^+$  are given in Ref. [29] and are repeated below:

$$\begin{aligned} B_{\mu^-\tau^+}^{B \rightarrow K} &= \left( (9.6 \pm 1.0) |C_9^{bs\mu\tau}(\text{NP})|^2 + (10.0 \pm 1.3) |C_{10}^{bs\mu\tau}(\text{NP})|^2 \right) \times 10^{-9} , \\ B_{\mu^-\tau^+}^{B \rightarrow K^*} &= \left( (19.4 \pm 2.9) |C_9^{bs\mu\tau}(\text{NP})|^2 + (18.1 \pm 2.6) |C_{10}^{bs\mu\tau}(\text{NP})|^2 \right) \times 10^{-9} . \end{aligned} \quad (7)$$

The branching ratios for  $B \rightarrow K^{(*)}\tau^-\mu^+$  are given by replacing  $bs\mu\tau$  with  $b\tau\mu$ .

- $\tau \rightarrow \mu\phi$ :

$$C_9^{ss\tau\mu}(\text{NP}) = -C_{10}^{ss\tau\mu}(\text{NP}) = -\frac{\pi}{\sqrt{2}\alpha G_F V_{tb} V_{ts}^*} \frac{(G_1 + G_3)^{ss\tau\mu}}{M_{\text{NP}}^2} .$$

The branching ratio is

$$B_{\tau^+\mu^+}^\phi = \frac{f_\phi^2 m_\tau^3}{128\pi \Gamma_\tau} (1 - r_\tau^{-1})^2 (1 + 2r_\tau^{-1}) \left[ |(G_1 + G_3)^{ss\tau\mu}|^2 + |(G_1 + G_3)^{s\tau\mu}|^2 \right] , \quad (8)$$

where  $r_\tau \equiv m_\tau^2/m_\phi^2$  and  $f_\phi = (238 \pm 3) \text{ MeV}$  [66].

Observable	Measurement or Constraint
minimal	
$b \rightarrow s\mu^+\mu^-$ (all)	$C_9^{\mu\mu}(\text{LQ}) = -C_{10}^{\mu\mu}(\text{LQ}) = -0.68 \pm 0.12$ [17]
$R_{D^*}^{\tau/\ell}/(R_{D^*}^{\tau/\ell})_{\text{SM}}$	$1.18 \pm 0.06$ [18–21]
$R_D^{\tau/\ell}/(R_D^{\tau/\ell})_{\text{SM}}$	$1.36 \pm 0.15$ [18–21]
$R_{D^*}^{e/\mu}/(R_{D^*}^{e/\mu})_{\text{SM}}$	$1.04 \pm 0.05$ [68]
$R_{J/\psi}^{\tau/\mu}/(R_{J/\psi}^{\tau/\mu})_{\text{SM}}$	$2.51 \pm 0.97$ [22]
$\mathcal{B}(B \rightarrow K^{(*)}\nu\bar{\nu})/\mathcal{B}(B \rightarrow K^{(*)}\nu\bar{\nu})_{\text{SM}}$	$-13 \sum_{i=1}^3 \text{Re}[C_L^{ii}(\text{LQ})] + \sum_{i,j=1}^3  C_L^{ij}(\text{LQ}) ^2 \leq 248$ [69]
LFV	
$\mathcal{B}(B^+ \rightarrow K^+\tau^-\mu^+)$	$(0.8 \pm 1.7) \times 10^{-5}$ ; $< 4.5 \times 10^{-5}$ (90% C.L.) [70]
$\mathcal{B}(B^+ \rightarrow K^+\tau^+\mu^-)$	$(-0.4 \pm 1.2) \times 10^{-5}$ ; $< 2.8 \times 10^{-5}$ (90% C.L.) [70]
$\mathcal{B}(\Upsilon(2S) \rightarrow \mu^\pm\tau^\mp)$	$(0.2 \pm 1.5 \pm 1.3) \times 10^{-6}$ ; $< 3.3 \times 10^{-6}$ (90% C.L.) [71]
$\mathcal{B}(\tau \rightarrow \mu\phi)$	$< 8.4 \times 10^{-8}$ (90% C.L.) [72]
$\mathcal{B}(J/\psi \rightarrow \mu^\pm\tau^\mp)$	$< 2.0 \times 10^{-6}$ (90% C.L.) [73]

TABLE I. Measured values or constraints of the  $2q2\ell$  observables that can significantly constrain the NP models.

- $\Upsilon(nS) \rightarrow \mu^\pm\tau^\mp$ : the branching ratio is

$$B_{\tau\mu}^{\Upsilon(nS)} = \frac{f_{\Upsilon(nS)}^2 m_{\Upsilon(nS)}^3}{48\pi \Gamma_{\Upsilon(nS)} M_{\text{NP}}^4} (2 + r'_\tau)(1 - r'_\tau)^2 \left[ |(G_1 + G_3)^{bb\mu\tau}|^2 + |(G_1 + G_3)^{bb\tau\mu}|^2 \right], \quad (9)$$

where  $r'_\tau \equiv m_\tau^2/m_{\Upsilon(nS)}^2$ ,  $f_{\Upsilon(1S)} = (700 \pm 16)$  MeV,  $f_{\Upsilon(2S)} = (496 \pm 21)$  MeV, and  $f_{\Upsilon(3S)} = (430 \pm 21)$  MeV [39].

- $J/\psi \rightarrow \mu^\pm\tau^\mp$ : the branching ratio is obtained from Eq. (9) by replacing  $\Upsilon \rightarrow J/\psi$  and  $(G_1 + G_3)^{bb\ell\ell'} \rightarrow [V(G_1 - G_3)V^\dagger]^{c\ell\ell'}$ , with  $f_{J/\psi} = (401 \pm 46)$  MeV [67].

Above, we identified the  $2q2\ell$  observables that can significantly constrain the NP models. We list these observables, along with their present measured values or constraints, in Table I.

Some comments concerning the entries in the Table may be useful:

- A fit to all  $b \rightarrow s\mu^+\mu^-$  data ( $B \rightarrow K^{(*)}\mu^+\mu^-$ ,  $B_s^0 \rightarrow \phi\mu^+\mu^-$ ,  $B_s^0 \rightarrow \mu^+\mu^-$ ,  $R_{K^{(*)}}$ ) was done in Ref. [17], leading to the constraint on  $C_9^{\mu\mu}(\text{LQ}) = -C_{10}^{\mu\mu}(\text{LQ})$  given in the Table.
- Similarly, the analysis of  $B \rightarrow K^{(*)}\nu\bar{\nu}$  decays done in Ref. [69] leads to the constraint on  $C_L^{ij}(\text{LQ})$  given in the Table. There is also an upper limit on  $\mathcal{B}(B_s^0 \rightarrow \phi\nu\bar{\nu})$ , but it is much weaker than that of  $\mathcal{B}(B \rightarrow K^{(*)}\nu\bar{\nu})$ .
- The results of the measurements of LFV processes are usually given in terms of 90% C.L. upper limits (ULs) on the branching ratios. For certain measurements ( $B^+ \rightarrow K^+\tau^-\mu^+$ ,  $B^+ \rightarrow K^+\tau^+\mu^-$ ,  $\Upsilon(2S) \rightarrow \mu^\pm\tau^\mp$ ) the actual central values and errors are given, in addition to the UL. These are extremely useful, as they can be included in a fit. For other measurements ( $\tau \rightarrow \mu\phi$ ,  $J/\psi \rightarrow \mu^\pm\tau^\mp$ ), only the UL is given. In order to include these measurements in a fit, we convert the ULs to a branching ratio of  $0 \pm \text{UL}/1.5$ .
- Other analyses combine  $\mathcal{B}(B \rightarrow K\tau^-\mu^+)$  and  $\mathcal{B}(B \rightarrow K\tau^+\mu^-)$ . However, in the case of LQ models, this is not correct, as the two decays involve different couplings.
- As we describe later, in this paper we assume that the NP does not couple significantly to the first-generation down-type quarks. However, it does couple to first-generation up-type quarks via the CKM matrix [Eq. (2)]. As a result, there is an additional LFV process to which the NP contributes at tree level:  $\tau \rightarrow \mu\rho^0$ . Experimentally, it is found that  $\mathcal{B}(\tau \rightarrow \mu\rho^0) < 1.2 \times 10^{-8}$  (90% C.L.) [72], which is stronger than the other upper limits in the Table. This said, it can be shown that the NP contribution to  $\tau \rightarrow \mu\rho^0$  is  $|V_{us}|^2 \simeq 0.05$  times that to  $\tau \rightarrow \mu\phi$ . As a result, the constraint from  $\tau \rightarrow \mu\rho^0$  is much weaker than that from  $\tau \rightarrow \mu\phi$ , and for this reason this LFV process is not included in the Table.

In LQ models, the only NP contributions are to the  $2q2\ell$  observables described above. On the other hand, in the  $VB$  model, there are also tree-level contributions to four-quark and four-lepton observables. The five additional observables that yield important constraints on the  $VB$  model are  $B_s^0$ - $\bar{B}_s^0$  mixing, neutrino trident production,  $\tau \rightarrow 3\mu$ ,  $\tau \rightarrow \mu\nu\bar{\nu}$  and  $D^0$ - $\bar{D}^0$  mixing. These will be discussed in more detail in Sec. IV.1.

### III. LEPTOQUARK MODELS

There are three types of leptoquarks that contribute to both  $b \rightarrow s\mu^+\mu^-$  and  $b \rightarrow c\tau^-\bar{\nu}$ . They are (i) an  $SU(2)_L$ -triplet scalar LQ ( $S_3$ )  $[(\mathbf{3}, \mathbf{3}, -2/3)]$ , (ii) an  $SU(2)_L$ -triplet vector LQ ( $U_3$ )  $[(\mathbf{3}, \mathbf{3}, 4/3)]$ , and (iii) an  $SU(2)_L$ -singlet vector LQ ( $U_1$ )  $[(\mathbf{3}, \mathbf{1}, 4/3)]$ . In the mass basis, their interaction Lagrangians are given by [74]

$$\begin{aligned}\Delta\mathcal{L}_{S_3} &= h_{ij}^{S_3} (\bar{Q}_{iL} \sigma^I i \sigma^2 L_{jL}^c) S_3^I + \text{h.c.}, \\ \Delta\mathcal{L}_{U_3} &= h_{ij}^{U_3} (\bar{Q}_{iL} \gamma^\mu \sigma^I L_{jL}) U_{3\mu}^I + \text{h.c.}, \\ \Delta\mathcal{L}_{U_1} &= h_{ij}^{U_1} (\bar{Q}_{iL} \gamma^\mu L_{jL}) U_{1\mu} + \text{h.c.}\end{aligned}\tag{10}$$

Note that the  $S_3$  coupling violates fermion number, while those of  $U_3$  and  $U_1$  are fermion-number conserving. When the heavy LQ is integrated out, we obtain the following effective Lagrangians:

$$\begin{aligned}\mathcal{L}_{S_3}^{\text{eff}} &= \frac{h_{ik} h_{jl}^*}{4M_{\text{LQ}}^2} [3 (\bar{Q}_{iL} \gamma^\mu Q_{jL}) (\bar{L}_{kL} \gamma_\mu L_{lL}) + (\bar{Q}_{iL} \gamma^\mu \sigma^I Q_{jL}) (\bar{L}_{kL} \gamma_\mu \sigma^I L_{lL})] , \\ \mathcal{L}_{U_3}^{\text{eff}} &= -\frac{h_{il} h_{jk}^*}{2M_{\text{LQ}}^2} [3 (\bar{Q}_{iL} \gamma^\mu Q_{jL}) (\bar{L}_{kL} \gamma_\mu L_{lL}) - (\bar{Q}_{iL} \gamma^\mu \sigma^I Q_{jL}) (\bar{L}_{kL} \gamma_\mu \sigma^I L_{lL})] , \\ \mathcal{L}_{U_1}^{\text{eff}} &= -\frac{h_{il} h_{jk}^*}{2M_{\text{LQ}}^2} [(\bar{Q}_{iL} \gamma^\mu Q_{jL}) (\bar{L}_{kL} \gamma_\mu L_{lL}) + (\bar{Q}_{iL} \gamma^\mu \sigma^I Q_{jL}) (\bar{L}_{kL} \gamma_\mu \sigma^I L_{lL})] .\end{aligned}\tag{11}$$

Comparing to Eq. (1), we see that  $G_1^{ijkl}$  is replaced by a constant  $g_1$  times the product of two LQ couplings  $h h^*$ , and similarly for  $G_3^{ijkl}$ . Note that, for the  $S_3$  model, the quarks are coupled to the opposite leptons than in the  $U_3$  and  $U_1$  models. This is due to the fact that the couplings violate ( $S_3$ ) or conserve ( $U_3$  and  $U_1$ ) fermion number, and is relevant only for lepton-flavour-violating processes. In the above, we have suppressed the LQ model labels on the couplings. The models are distinguished by their relative weighting of the two operators,  $g_1$  and  $g_3$ . These are

$$\begin{aligned}S_3 : g_1 &= 3g_3 = \frac{3}{4} , \\ U_3 : g_1 &= -3g_3 = -\frac{3}{2} , \\ U_1 : g_1 &= g_3 = -\frac{1}{2} .\end{aligned}\tag{12}$$

In this paper, we take the couplings to be real. In addition, since the  $b \rightarrow s\mu^+\mu^-$  and  $b \rightarrow c\tau^-\bar{\nu}$  anomalies involve only the second and third generations, for simplicity we assume that the LQ couplings to the first-generation leptons and down-type quarks are negligible in the mass basis<sup>2</sup>. (Even so, they couple to first-generation up-type quarks via the CKM matrix, see Eq. (2).)

In the following subsections, we confront the three LQ models with the data. For each of the models, we aim to answer two questions. Can the model explain the  $B$ -decay anomalies? If so, taking into account all constraints from  $2q2\ell$  observables, what ranges of couplings are allowed?

#### III.1. $S_3$ and $U_3$ LQs

For both the  $S_3$  and  $U_3$  LQ models, we perform a fit to the data using only the 6 minimal constraints of Table I and setting  $M_{\text{LQ}} = 1$  TeV. The theoretical parameters are the 4 couplings  $h_{22}$ ,  $h_{23}$ ,  $h_{32}$  and  $h_{33}$ , so that the number of degrees of freedom (d.o.f.) is 2.

In the SM,  $\chi_{\text{SM}}^2 = 52$ . We find  $\chi_{\text{min, SM}+S_3}^2 = 15$ , so the addition of the  $S_3$  LQ does indeed improve things. On the other hand, the  $\chi_{\text{min}}^2/\text{d.o.f.} = 7.5$ . An acceptable fit has  $\chi_{\text{min}}^2/\text{d.o.f.} \simeq 1$ , so that, even with the addition of the NP, the fit is still very poor. Thus, the  $S_3$  LQ model cannot explain the  $B$ -decay anomalies. (In Ref. [49], the  $S_3$  LQ was allowed to couple to both the second and third generations, and the same result was found.)

The analysis of the  $U_3$  LQ model is similar. The fit to the 6 minimal constraints yields  $\chi_{\text{min, SM}+U_3}^2 = 20$ , or  $\chi_{\text{min}}^2/\text{d.o.f.} = 10$ . Here too the fit is very poor: the  $B$ -decay anomalies cannot be explained in the  $U_3$  LQ model either.

<sup>2</sup> For discussions of processes that are affected if there are also nonzero first-generation couplings, see Refs. [75, 76], for example.

For both LQs we can understand why this is so. The constraint from the  $b \rightarrow s\mu^+\mu^-$  data implies  $(g_1 + g_3)h_{32}h_{22} = 0.0011 \pm 0.0002$  for  $M_{\text{LQ}} = 1$  TeV, while that from  $R_{D^{(*)}}$  leads to  $2g_3h_{33}h_{23} = -0.14 \pm 0.04$ . There are several NP contributions to  $B \rightarrow K^{(*)}\nu\bar{\nu}$ , leading to different flavours of the final-state neutrinos. However, the most important ones are those that lead to processes that also appear in the SM. The reason is that, due to SM-NP interference, there are linear NP terms in the matrix element. There are two possibilities for the neutrinos:  $\nu_\mu\bar{\nu}_\mu$  and  $\nu_\tau\bar{\nu}_\tau$ , whose NP contributions involve  $h_{32}h_{22}$  and  $h_{33}h_{23}$ , respectively. However, from the above constraints we have  $|h_{32}h_{22}| \ll |h_{33}h_{23}|$ , so that the NP contribution to  $B \rightarrow K^{(*)}\nu\bar{\nu}$  is dominated by  $b \rightarrow s\nu_\tau\bar{\nu}_\tau$ . The constraint from  $B \rightarrow K^{(*)}\nu\bar{\nu}$  then leads to  $-0.047 \leq (g_1 - g_3)h_{33}h_{23} \leq 0.026$ . For the  $S_3$  LQ, we have  $h_{33}h_{23} = -0.28 \pm 0.08$  ( $R_{D^{(*)}}$ ) and  $h_{33}h_{23} \geq -0.094$  ( $B \rightarrow K^{(*)}\nu\bar{\nu}$ ). Similarly, the  $U_3$  LQ has  $h_{33}h_{23} = -0.14 \pm 0.04$  ( $R_{D^{(*)}}$ ) and  $h_{33}h_{23} \geq -0.013$  ( $B \rightarrow K^{(*)}\nu\bar{\nu}$ ). In both cases, the two constraints on  $h_{33}h_{23}$  are incompatible, so that the  $S_3$  and  $U_3$  LQ models cannot explain the  $B$ -decay data.

Previous analyses [39, 50] ruled out the  $S_3$  and  $U_3$  models as candidate for explaining all the  $B$ -decay anomalies. In these papers it was assumed that the NP couples predominantly to the third generation. We have shown that the elimination of these models is completely general – even if the NP couplings involving the second generation are allowed to be sizeable, the  $S_3$  and  $U_3$  LQ models still cannot explain the  $b \rightarrow s\mu^+\mu^-$  and  $b \rightarrow c\tau^-\bar{\nu}$  anomalies.

## III.2. $U_1$ LQ

### III.2.1. Fit

For the  $U_1$  LQ, we perform a fit to all the  $2q2\ell$  observables in Table I, again taking  $M_{\text{LQ}} = 1$  TeV. There are two important details. First, for  $\tau \rightarrow \mu\phi$  there is only a 90% C.L. upper limit on its branching ratio of  $8.4 \times 10^{-8}$ . In order to incorporate this observable into the fit, we take  $\mathcal{B}(\tau \rightarrow \mu\phi) = (0.0 \pm 5.6) \times 10^{-8}$ . Second, note that the contribution to  $b \rightarrow s\nu\bar{\nu}$  vanishes if  $g_1 = g_3$  [see  $C_L^{ij}$  (NP) in Eq. (6)]. But this is precisely the definition of the  $U_1$  model [Eq. (12)], so there are no constraints on the  $U_1$  LQ from this process. This avoids the problem that eliminated the  $S_3$  and  $U_3$  LQ models. Similarly, the  $U_1$  LQ does not contribute to  $J/\psi \rightarrow \mu^\pm\tau^\mp$ . There are thus 9 observables in the fit. As before, the theoretical parameters are  $h_{22}$ ,  $h_{23}$ ,  $h_{32}$  and  $h_{33}$ , so that the d.o.f. is 5.

We find  $\chi_{\min, \text{SM}+U_1}^2 = 5.0$ , or  $\chi_{\min}^2/\text{d.o.f.} = 1.0$ . This is an acceptable fit, so we see that the  $U_1$  LQ model does provide an explanation of the  $B$ -decay anomalies.

Now, the observables depend almost exclusively on products of the couplings:

$$\begin{aligned} b \rightarrow s\mu^+\mu^- : h_{32}h_{22} , \\ b \rightarrow c\tau^-\bar{\nu} : V_{cs}h_{33}h_{23} + V_{cb}h_{33}^2 , \\ B^+ \rightarrow K^+\tau^-\mu^+ : h_{32}h_{23} , \\ B^+ \rightarrow K^+\tau^+\mu^- : h_{33}h_{22} , \\ \Upsilon(2S) \rightarrow \mu^\pm\tau^\mp : h_{33}h_{32} , \\ \tau \rightarrow \mu\phi : h_{23}h_{22} . \end{aligned} \tag{13}$$

The only term that depends on a single coupling is the  $h_{33}^2$  contribution in  $b \rightarrow c\tau^-\bar{\nu}$ . But since it is multiplied by the small CKM matrix element  $V_{cb}$ , its effect is small (unless  $h_{33}$  is quite large). And because only products of couplings are involved, there is little information about the individual couplings themselves.

This is illustrated in Fig. 1, where we show the allowed 95% C.L. regions in  $h_{33}$ - $h_{23}$  space (left plot)<sup>3</sup> and in  $h_{32}$ - $h_{22}$  space (right plot). These regions are determined largely by the  $b \rightarrow c\tau^-\bar{\nu}$  and  $b \rightarrow s\mu^+\mu^-$  data, respectively. When one adds the LFV constraints, the allowed regions are reduced in size, but are still sizeable. The LFV constraints place maximal values on some of the couplings:  $|h_{22}| \leq 0.12$ ,  $|h_{32}| \leq 0.7$ , and  $h_{23} \leq 0.9$ . They also lead to  $h_{33} \geq 0.1$ .

Some additional information can be learned by performing fits with fixed values of  $h_{33}$ . In Table II, we present  $\chi_{\min, \text{SM}+U_1}^2$  and the best-fit value of  $h_{23}$  for various values of  $h_{33}$ . We see that, as  $h_{33}$  decreases and  $h_{23}$  increases,  $\chi_{\min, \text{SM}+U_1}^2$  increases. This indicates that the data prefer larger values of  $h_{33}$  and smaller values of  $h_{23}$ .

But this all raises a question. In the fit, we have seen that the LFV constraints put maximal values on some of the couplings. Is this the only effect of the LFV observables? The answer is no. Because the LFV processes of Eq. (13) involve one of  $\{h_{33}, h_{23}\}$  and one of  $\{h_{32}, h_{22}\}$ , they relate portions of the  $h_{33}$ - $h_{23}$  and  $h_{32}$ - $h_{22}$  regions. And, in fact, these relations can be quite important.

<sup>3</sup> In order for the  $h_{ij}$  to be perturbative, we must have  $h_{ij}^2/4\pi < 1$ . To ensure this, we take the maximal value of the couplings to be  $|h_{ij}| = 1$ .

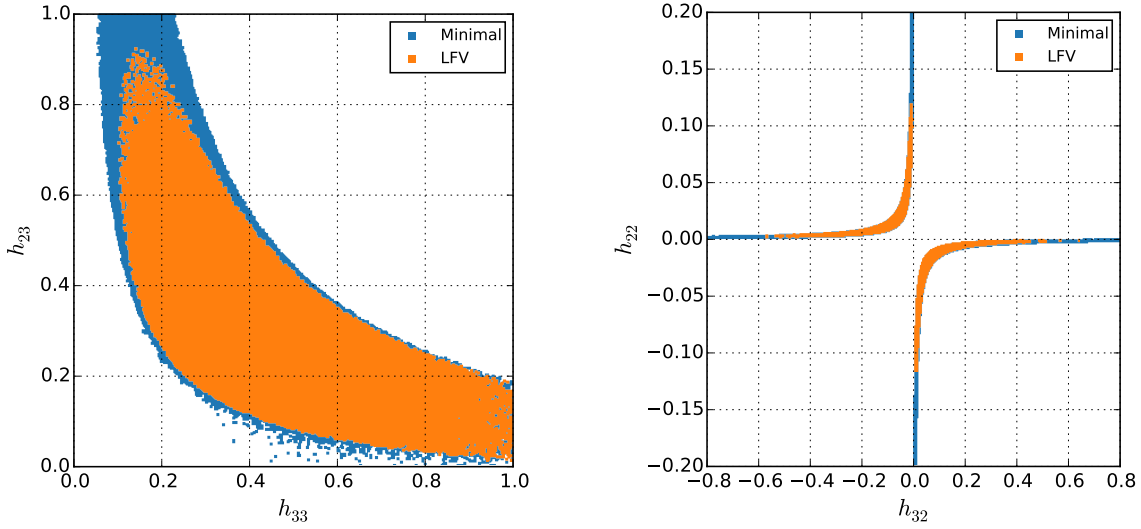


FIG. 1. Allowed 95% C.L. regions in  $h_{33}$ - $h_{23}$  space (left plot) and  $h_{32}$ - $h_{22}$  space (right plot), for  $M_{\text{LQ}} = 1$  TeV. The regions are shown for a fit with only minimal constraints (blue) or minimal + LFV constraints (orange).

$h_{33}$	$\chi^2_{\text{min}, \text{SM}+U_1}$	$h_{23}$
1.0	5.0	$0.10 \pm 0.04$
0.5	5.2	$0.26 \pm 0.07$
0.2	6.8	$0.60 \pm 0.15$
0.1	11.3	$0.70 \pm 0.20$

TABLE II.  $U_1$  LQ model:  $\chi^2_{\text{min}, \text{SM}+U_1}$  and the best-fit value of  $h_{23}$  for various values of  $h_{33}$ , for  $M_{\text{LQ}} = 1$  TeV.

To illustrate this, we note that the  $b \rightarrow c\tau^-\bar{\nu}$  data imply  $h_{33}h_{23} = 0.14 \pm 0.04 = O(0.1)$  for  $M_{\text{LQ}} = 1$  TeV. To reproduce this, we consider two limiting cases:  $\{h_{33}, h_{23}\} =$  (a)  $\{0.1, 1.0\}$  or (b)  $\{1.0, 0.1\}$ . Also, the  $b \rightarrow s\mu^+\mu^-$  data lead to  $h_{32}h_{22} = -0.0011 \pm 0.0002 = O(0.001)$ . In the same vein, we consider two limiting cases:  $\{h_{32}, h_{22}\} =$  (c)  $\{O(0.01), O(0.1)\}$  or (d)  $\{O(0.1), O(0.01)\}$ . These can be combined to produce four rough scenarios for the four couplings:

$$\begin{aligned}
A &= (a, c) : h_{33} = O(1.0) , \quad h_{23} = O(0.1) , \quad h_{32} = O(0.01) , \quad h_{22} = O(0.1) , \\
B &= (b, c) : h_{33} = O(0.1) , \quad h_{23} = O(1.0) , \quad h_{32} = O(0.01) , \quad h_{22} = O(0.1) , \\
C &= (a, d) : h_{33} = O(1.0) , \quad h_{23} = O(0.1) , \quad h_{32} = O(0.1) , \quad h_{22} = O(0.01) , \\
D &= (b, d) : h_{33} = O(0.1) , \quad h_{23} = O(1.0) , \quad h_{32} = O(0.1) , \quad h_{22} = O(0.01) .
\end{aligned} \tag{14}$$

We now repeat the fit, fixing the couplings  $h_{33}$  and  $h_{23}$  as per (a) or (b). In addition, the fit is performed using (i) only the minimal constraints or (ii) the minimal + LFV constraints. The allowed 95% C.L. regions in  $h_{32}$ - $h_{22}$  space are shown in Fig. 2, with case (a) on the left and case (b) on the right. If only minimal constraints are used, there is no difference between (a) and (b) – the allowed region is the same in both cases, and scenarios  $A$ ,  $B$ ,  $C$  and  $D$  are all allowed. However, this changes when the LFV constraints are added. For case (a), the allowed region is greatly reduced:  $h_{32}$  and  $h_{22}$  must both be rather small, and scenarios  $B$  and  $D$  are both ruled out. On the other hand, the effect of the addition of the LFV constraints is much less dramatic for case (b). Most of the region allowed with minimal constraints is still allowed, though scenario  $A$  is now ruled out. This demonstrates the effect that the LFV constraints have on the parameter space.

We have emphasized that previous analyses made the theoretical assumption that the NP couples predominantly to the third generation. This implies a large value of  $h_{33}$ . Now, above we noted that the data prefer larger values of  $h_{33}$ . This suggests that, in fact, such a theoretical assumption is not necessary – the data point in this direction. How does this come about? After all, the  $b \rightarrow c\tau^-\bar{\nu}$  constraints depend essentially on the product  $h_{33}h_{23}$  [Eq. (13)]. So a small value of  $h_{33}$  can be compensated for by a large value of  $h_{23}$ . However, we saw above that such a scenario is disfavoured by the LFV constraints. Indeed, it is these LFV constraints that lead to the requirement of a large value



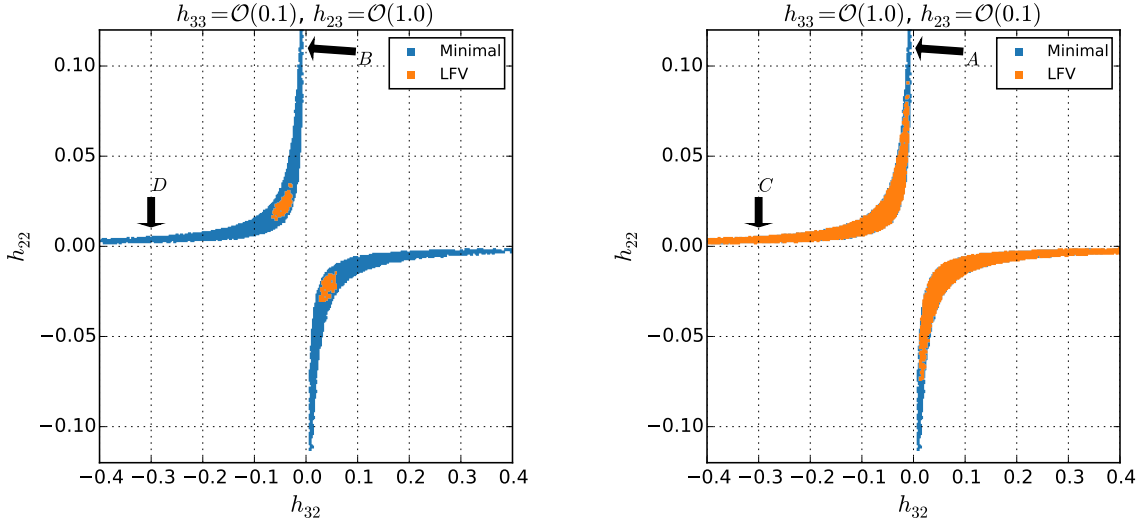


FIG. 2. Allowed 95% C.L. region in  $h_{32}$ - $h_{22}$  space for  $\{h_{33}, h_{23}\} = \{O(0.1), O(1.0)\}$  (left plot) or  $\{h_{33}, h_{23}\} = \{O(1.0), O(0.1)\}$  (right plot), for  $M_{LQ} = 1$  TeV. The region is shown for a fit with only minimal constraints (blue) or minimal + LFV constraints (orange).

of  $h_{33}$ , in line with the theoretical assumption.

### III.2.2. Renormalization group equations

In Refs. [35, 47], additional constraints were derived. The starting point is the observation that the scale of NP,  $\Lambda$ , is well above the weak scale  $v$  [e.g.,  $\Lambda = O(\text{TeV})$ ]. Below  $\Lambda$ , but above  $v$ , the physics is described by  $\mathcal{L}_{\text{SM}} + \mathcal{L}_{\text{NP}}$ . Here  $\mathcal{L}_{\text{NP}}$  is the effective Lagrangian obtained when the NP is integrated out; it is invariant under the SM gauge group. In Refs. [35, 47], it was assumed that the dominant terms in  $\mathcal{L}_{\text{NP}}$  are the  $2q2\ell$  operators of Eq. (1), written in the weak basis, with the NP coupling only to the third generation. Once  $SU(2)_L \times U(1)_Y$  is broken, the fermions acquire masses. One transforms from the weak basis to the mass basis by acting on the fermion fields with unitary transformations. In the mass basis, the NP couplings are functions of these transformations and the couplings in the weak basis.

$\mathcal{L}_{\text{NP}}$  is evolved from the NP scale  $\Lambda$  to the weak scale using the one-loop renormalization group equations (RGEs) in the limit of exact electroweak symmetry. After performing a matching at the weak scale, it is further evolved down to the scale of 1 GeV using the QED RGEs and integrating out the heavy degrees of freedom.

This evolution has several effects. First, for the  $U_1$  LQ model, recall that the constraints from  $b \rightarrow s\nu\bar{\nu}$  could be evaded because  $g_1 = g_3$ . However, this equality holds only at the NP scale  $\Lambda$ . At lower energies, a nonzero value of  $\delta g_- \equiv g_1 - g_3$  is generated. This means that constraints from  $B \rightarrow K^{(*)}\nu\bar{\nu}$  must be taken into account for  $U_1$ .

Second, there is operator mixing during the RGE evolution. One of the effects is that the leptonic couplings of the  $W^\pm$  and  $Z^0$  are modified. This can be understood as follows. If one combines the SM decay  $Z^0 \rightarrow q\bar{q}$  with the NP process  $q\bar{q} \rightarrow \ell_i\bar{\ell}_j$ , this corresponds to a (loop-level) NP contribution to  $Z^0 \rightarrow \ell_i\bar{\ell}_j$ . If  $i = j$ , this is a correction to the coupling of the  $Z^0$  to charged or neutral leptons. And if  $i \neq j$ , this generates an LFV decay of the  $Z^0$ . There are similar effects for the coupling of the  $Z^0$  to quarks, and all this also holds for the  $W^\pm$ . However, since the leptonic couplings of the  $Z^0$  are the most precisely measured, the constraints from these measurements are the most important.

Another effect of this operator mixing is that, at low energies, when the  $W$ ,  $Z$ ,  $t$ ,  $b$  and  $c$  have all been integrated out, one generates four-fermion LFV processes such as  $\tau \rightarrow 3\mu$ ,  $\tau \rightarrow \mu\rho$  and  $\tau \rightarrow \mu\pi$ , as well as corrections to the LFC decay  $\tau \rightarrow \ell\nu_\tau\bar{\nu}_\ell$ . In the case of  $\tau \rightarrow 3\mu$ , this can be understood as the combination of SM  $q\bar{q}\mu^+\mu^-$  and NP  $q\bar{q}\mu\tau$  operators.

Two scenarios are examined in Ref. [35]: (i)  $g_1 = 0$  and  $|g_3| \leq 3$ , (ii)  $g_1 = g_2$ . It is argued that the new RGE constraints are very important, particularly for scenario (i). In Ref. [47], under the additional assumptions that the mass-basis couplings obey  $h_{33} = 1$ ,  $h_{23} = h_{32}$  and  $h_{22} = h_{23}^2$ , it was shown that the RGE constraints rule out scenario (ii) entirely, mostly due to the constraints from  $\tau \rightarrow \ell\nu\bar{\nu}$ . (We note that the assumptions about the couplings correspond to an extremely special case, where the transformations from the weak to the mass basis are the same for

down-type quarks and charged leptons.)

We have several observations regarding the above RGE analysis:

- The analysis of Refs. [35, 47] is at the level of an effective field theory (EFT). As such, the results of this analysis are not necessarily applicable to all models, since a given model may have additional operators in  $\mathcal{L}_{\text{NP}}$ . These extra operators may affect the RGEs and the conclusions.
- As a specific example, the  $VB$  model has  $g_1 = 0$ , and so one might think it is represented by scenario (i) above. This is not true: the  $VB$  model also has tree-level four-quark and four-lepton operators. In particular, there is a tree-level contribution to  $\tau \rightarrow 3\mu$ . In this case, the RGE generation of a (loop-level) contribution to  $\tau \rightarrow 3\mu$  is irrelevant.
- A similar comment applies to the EFT analysis itself. Much emphasis is placed on the RGE generation of contributions to LFV processes such as  $\tau \rightarrow 3\mu$ ,  $\tau \rightarrow \mu\rho$ , etc. However, all of these processes arise due to the combination of a SM operator with the NP operator  $(\bar{q}_{iL}\gamma_\mu q_{jL})(\bar{\mu}_L\gamma^\mu\tau_L)$ . But the very existence of this NP operator leads to tree-level LFV effects in  $B \rightarrow K\tau\mu$ ,  $\tau \rightarrow \mu\phi$ ,  $\Upsilon \rightarrow \mu\tau$  and  $J/\psi \rightarrow \mu\tau$ . There are stringent upper bounds on the branching ratios of all of these processes (see Table I). The upshot is that there is no need to consider the loop-level RGE effects – the constraints on the NP operator coming from these tree-level processes are stronger.
- Finally, the EFT analysis also leads to NP contributions to LFC processes such as  $Z^0 \rightarrow \ell^+\ell^-$ ,  $Z^0 \rightarrow \nu_\ell\bar{\nu}_\ell$  and  $\tau \rightarrow \ell\nu_\tau\bar{\nu}_\ell$ . These processes are all measured quite precisely, so that, even though the NP contributions are small (loop level), they can be constrained by the measurements. While this conclusion is valid for the EFT, it does not necessarily hold in a real model. Consider the  $U_1$  LQ. It contributes at one loop to all of these processes, so that, once the NP is integrated out, there are new operators in  $\mathcal{L}_{\text{NP}}$ . Compared to the  $2q2\ell$  operators of Eq. (1), they are indeed subdominant. However, they are of the same order as the low-energy RGE effects, so that there may be a partial cancellation between the two contributions. The bottom line is that the RGE constraints from LFC processes must be taken with a grain of salt – they may be evaded in real models. (To be fair, this is acknowledged explicitly in Ref. [47].)

Our conclusion is that, while the RGE analysis of Refs. [35, 47] is interesting, the results are suspect because the tree-level LFV constraints have not been properly taken into account. And even if they are, one has to be very careful about taking its constraints too literally, as they may not hold in real models.

This said, in order to compare with previous analyses, we apply the RGE analysis to our  $U_1$  model, taking  $M_{\text{LQ}} = 1$  TeV. In our general study, (i) we do not assume that the NP couples only to the third generation in the weak basis, and (ii) we work in the mass basis. In order to repeat the RGE analysis, but with our setup, we use the programs `Wilson` [84] and `flavio` [85]. The RGE constraints arise from the contributions to LFV  $\tau$  decays,  $Z$ -pole observables and  $\tau \rightarrow \ell\nu_\tau\bar{\nu}_\ell$  ( $\ell = e, \mu$ ). (Note that we have verified that `Wilson` and `flavio` reproduce previous calculations of the RGE constraints [47, 50].)

In Fig. 3, we show the allowed 95% C.L. regions in  $h_{33}$ - $h_{23}$  space (left plot) and in  $h_{32}$ - $h_{22}$  space (right plot), when the RGE (green) or LFV (orange) constraints are added to the minimal constraints<sup>4</sup>. One sees from these plots that, in general, the LFV constraints are more stringent than the RGE constraints. For example, the LFV constraints lead to  $|h_{22}| \leq 0.12$ ,  $|h_{32}| \leq 0.7$ , and  $h_{23} \leq 0.9$ , whereas the RGE constraints allow all of these couplings to be as large as 1. Also, one has  $h_{33} \geq 0.1$  with the LFV constraints, while the RGE constraints allow this coupling to be slightly smaller. The only coupling value for which this behaviour does not hold is the maximal value of  $h_{33}$ . The RGE constraints require  $h_{33} \leq 1.3$ , while the LFV constraints allow much larger values. This said, such large couplings are entering the nonperturbative regime, which is why we previously imposed an upper limit of 1 on the absolute value of all couplings. Thus, if one requires  $|h_{ij}| \leq 1$ , the RGE constraints are irrelevant compared to the LFV constraints.

### III.2.3. $B_s^0$ - $\bar{B}_s^0$ mixing

In Sec. III.2.2 above, we saw that the  $U_1$  LQ can contribute at one loop to four-lepton operators, and there can potentially be some constraints from the measurements of such processes. In the same vein, there can also be one-loop contributions to four-quark processes. From the point of view of constraining the  $U_1$  model, the most promising

<sup>4</sup> We note that, if one compares Fig. 3 with the equivalent figure in Ref. [50], the regions with RGE constraints don't look the same. However, this is because different notations are used. We vary the couplings  $h_{ij}$  ( $ij = 22, 23, 32, 33$ ), while the couplings in Ref. [50] are  $g_U\beta_{ij}$  ( $ij = 22, 23, 32, 33$ ), with  $\beta_{33}$  fixed to 1 and the coupling constant  $g_U$  allowed to vary. If one takes into account this change of notation, it is found that the region with RGE constraints is very similar in the two analyses.

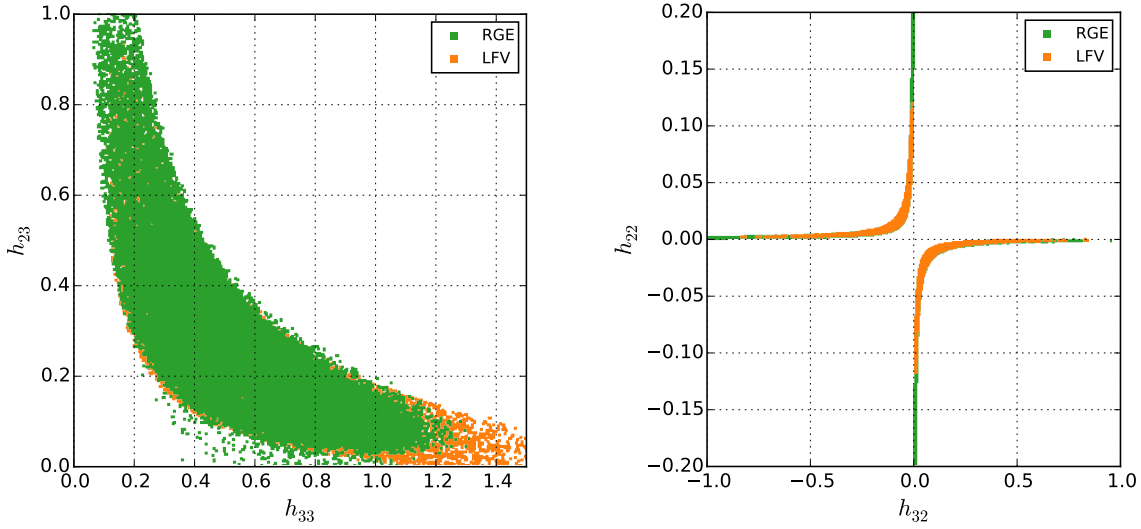


FIG. 3. Allowed 95% C.L. regions in  $h_{33}$ - $h_{23}$  space (left plot) and  $h_{32}$ - $h_{22}$  space (right plot), for  $M_{\text{LQ}} = 1$  TeV. The regions are shown for a fit with minimal + LFV constraints (orange) or minimal + RGE constraints (green).

four-quark observable is  $B_s^0$ - $\bar{B}_s^0$  mixing. Does its measurement, characterized by  $\Delta M_s$ , yield constraints on the  $U_1$  LQ?

In the SM, the underlying quark-level process can be accurately computed. However, there is a hadronic uncertainty in converting this to the level of mesons. This is described in detail in Sec. IV.1, but here we summarize the main points. The relevant hadronic parameter is  $f_{B_s} \sqrt{\hat{B}_{B_s}} = (266 \pm 18)$  MeV [86]. The central value is such that the SM reproduces the measured value of  $\Delta M_s$ . However, the error is sufficiently large that there is some room for NP. As a consequence, a small, loop-level NP contribution is allowed. That is, there are no constraints on the  $U_1$  LQ model from  $B_s^0$ - $\bar{B}_s^0$  mixing.

Recently, the hadronic parameters were recalculated, and larger values were found [87]. The implications for  $B_s^0$ - $\bar{B}_s^0$  mixing were examined in Ref. [88]. It was found that the central value of the SM prediction for  $\Delta M_s$  is now  $1.8\sigma$  above its measured value. This led the authors of Ref. [88] to observe that this poses problems for NP solutions of the  $b \rightarrow s\mu^+\mu^-$  anomalies. The point is that, regardless of whether the NP is a  $Z'$  or a LQ, the contribution to  $\Delta M_s$  has the same sign as that of the SM. That is, the discrepancy with measurement increases in the presence of NP. The problem is particularly severe for the  $Z'$ , where the contribution to  $B_s^0$ - $\bar{B}_s^0$  mixing is tree level, and hence large. But it also applies to the LQ, whose contribution is loop level.

If this new calculation is correct, it does indeed create problems for NP solutions of the  $B$  anomalies. But it also creates important problems for the SM. The SU(3)-breaking ratio of hadronic matrix elements in the  $B_s^0$  and  $B^0$  systems is well known:  $\xi = 1.206 \pm 0.018 \pm 0.006$  [87]. If the SM prediction of  $\Delta M_s$  is in disagreement with its measured value, the same holds for  $\Delta M_d$ . And this has important consequences for fits to the CKM matrix [89].

Thus, the results of the new calculation of the hadronic parameters may have important implications for the SM. In light of this, we prefer to wait for a verification of the new result before including it among the constraints on the  $U_1$  LQ model.

### III.3. Predictions

Having established that the  $U_1$  LQ model can explain the  $B$  anomalies, the next step is to examine ways of testing this explanation. To this end, here we present the predictions of the model.

Above, we have emphasized the importance of the semileptonic LFV processes  $B \rightarrow K^{(*)}\mu^\pm\tau^\mp$ ,  $\tau \rightarrow \mu\phi$  and  $\Upsilon \rightarrow \mu\tau$ . To date, no such decay has been observed. However, this may change in the future. For example, the expected reach of Belle II is  $\mathcal{B}(B^+ \rightarrow K^+\mu^\pm\tau^\mp) = 3.3 \times 10^{-6}$ ,  $\mathcal{B}(\Upsilon \rightarrow \mu^\pm\tau^\mp) = 1.0 \times 10^{-7}$  and  $\mathcal{B}(\tau \rightarrow \mu\phi) = 1.5 \times 10^{-9}$  [90]. Does the  $U_1$  model predict that at least one of these decays will be observed at Belle II? Unfortunately, the answer is no. In Fig. 4, we show the allowed 95% C.L. regions in  $h_{33}$ - $h_{23}$  space (left plot) and in  $h_{32}$ - $h_{22}$  space (right plot) for the case where *no* LFV signal is observed, i.e., where the above reaches are applied as upper limits. As can be seen from the figures, although the allowed space of couplings would be reduced, it is still sizeable. That is, if the

$U_1$  LQ model is the correct explanation of the  $B$  anomalies, an LFV process may be observed at Belle II, but there is no guarantee.

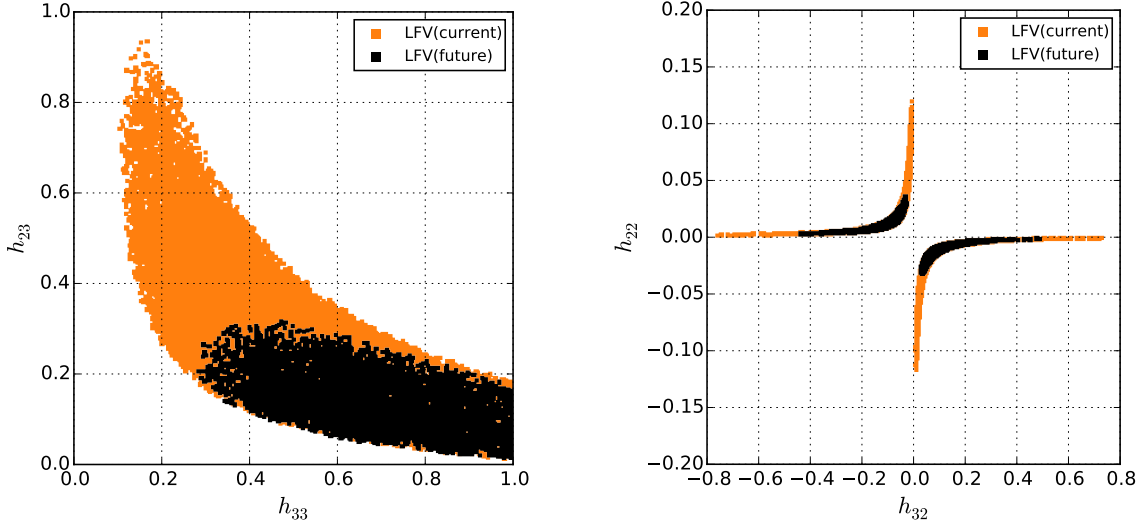


FIG. 4. Allowed 95% C.L. regions in  $h_{33}$ - $h_{23}$  space (left plot) and  $h_{32}$ - $h_{22}$  space (right plot), for  $M_{LQ} = 1$  TeV. The regions are shown for a fit with the minimal constraints + present LFV constraints (orange) or future LFV constraints (black).

Other observables are more promising. The measurement of  $R_{D^{(*)}}$  corresponds to LFUV in  $b \rightarrow c\ell^-\bar{\nu}_\ell$ . The NP effect is mainly for  $\ell = \tau$  and is governed by  $V_{cs}h_{33}h_{23} + V_{cb}h_{33}^2$  [Eq. (13)]. One then also expects to observe LFUV in  $b \rightarrow u\ell^-\bar{\nu}_\ell$ , with the NP contribution proportional to  $V_{us}h_{33}h_{23} + V_{ub}h_{33}^2$ . Such an effect can be seen in  $B \rightarrow \pi\ell\bar{\nu}_\ell$  or  $B^- \rightarrow \ell\bar{\nu}_\ell$  decays [91]. The observables are denoted  $R_{\pi\ell\bar{\nu}}^{\tau/\mu}$  and  $R_{\ell\bar{\nu}}^{\tau/\mu}$ , respectively. Another process where one expects significant NP effects is  $b \rightarrow s\tau^+\tau^-$ . Here the decays are  $B \rightarrow K^{(*)}\tau^+\tau^-$  and  $B_s^0 \rightarrow \tau^+\tau^-$ . Finally, there is  $B \rightarrow K^{(*)}\nu\bar{\nu}$ , whose fermion-level decay is  $b \rightarrow s\nu\bar{\nu}$ . As discussed in Sec. III.2.2, at low-energies there is a contribution to this decay from the  $U_1$  LQ, due to the evolution of the RGEs. As noted in Sec. III.2.2, one must take this calculation with a grain of salt, since there may be additional contributing operators at the NP scale.

The predictions for all these observables are shown in Fig. 5 as a function of the value of  $R_{D^{(*)}}^{\tau/\ell}/(R_{D^{(*)}}^{\tau/\ell})_{\text{SM}}$ , for  $M_{LQ} = 1$  TeV. For all three observables, there may be a significant enhancement compared to the SM predictions.  $R_{\pi\ell\bar{\nu}}^{\tau/\mu}$  and  $R_{\ell\bar{\nu}}^{\tau/\mu}$  can be larger by as much as 40%, while  $\mathcal{B}(B \rightarrow K^{(*)}\nu\bar{\nu})$  may be increased by 70% over the SM. As for  $\mathcal{B}(B \rightarrow K^{(*)}\tau^+\tau^-)$  and  $\mathcal{B}(B_s^0 \rightarrow \tau^+\tau^-)$ , they can be enhanced by as much as three orders of magnitude. This is consistent with the findings of Refs. [27, 44, 54]. (Ref. [92] discusses using  $b \rightarrow s\tau^+\tau^-$  to search for NP.)

One key feature of Fig. 5 is that these predictions are correlated with one another, and with the value of  $R_{D^{(*)}}^{\tau/\ell}/(R_{D^{(*)}}^{\tau/\ell})_{\text{SM}}$ . The reason is that the NP contributions to all four observables are either dominated by  $h_{23}h_{33}$  ( $b \rightarrow s\tau^+\tau^-$ ,  $b \rightarrow s\nu\bar{\nu}$ ) or have  $h_{23}h_{33}$  as the main component ( $b \rightarrow c\ell^-\bar{\nu}_\ell$ ,  $b \rightarrow u\ell^-\bar{\nu}_\ell$ ). Now,  $R_{D^{(*)}}^{\tau/\ell}$  will be remeasured with greater precision. If the deviation of its value from the SM prediction is found to be large (small), the deviations of the other observables from their SM predictions are also predicted to be large (small). This is a good test of the  $U_1$  LQ model.

#### IV. VECTOR BOSON MODEL

This model contains SM-like vector bosons ( $VB$ s) that transform as  $(\mathbf{1}, \mathbf{3}, 0)$  under  $SU(3)_C \times SU(2)_L \times U(1)_Y$ . The  $VB$ s are denoted  $V = W', Z'$ . In the mass basis, the Lagrangian describing the couplings of the  $VB$ s to left-handed fermions is

$$\Delta\mathcal{L}_V = g_{ij}^q (\bar{Q}_{iL} \gamma^\mu \sigma^I Q_{jL}) V_\mu^I + g_{ij}^\ell (\bar{L}_{iL} \gamma^\mu \sigma^I L_{jL}) V_\mu^I. \quad (15)$$

Integrating out the heavy  $VB$ s, we obtain the following effective Lagrangian, relevant for  $2q2\ell$  decays:

$$\mathcal{L}_V^{\text{eff}} = -\frac{g_{ij}^q g_{kl}^\ell}{M_V^2} (\bar{Q}_{iL} \gamma^\mu \sigma^I Q_{jL}) (\bar{L}_{kL} \gamma_\mu \sigma^I L_{lL}). \quad (16)$$

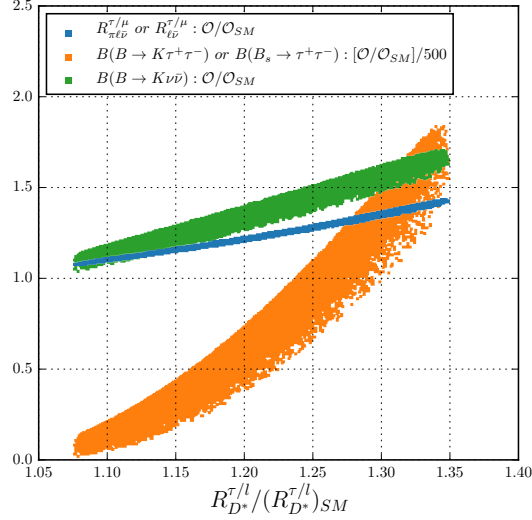


FIG. 5. Within the  $U_1$  LQ model with  $M_{LQ} = 1$  TeV, predictions for observables as a function of the value of  $R_{D^*}^{\tau/\ell}/(R_{D^*}^{\tau/\ell})_{SM}$ . Observables  $\mathcal{O}$  are:  $R_{\pi\ell\nu}^{\tau/\mu}$  or  $R_{\ell\nu}^{\tau/\mu}$  (blue),  $\mathcal{B}(B \rightarrow K^{(*)}\tau^+\tau^-)$  or  $\mathcal{B}(B_s^0 \rightarrow \tau^+\tau^-)$  (orange), and  $\mathcal{B}(B \rightarrow K^{(*)}\nu\bar{\nu})$  (green). Quantities plotted are  $\mathcal{O}/\mathcal{O}_{SM}$  (blue and green) or  $[\mathcal{O}/\mathcal{O}_{SM}]/500$  (orange).

Comparing this with Eq. (1), we find

$$G_1^{ijkl} = 0 \quad , \quad G_3^{ijkl} = -g_{ij}^q g_{kl}^\ell . \quad (17)$$

As was done with the LQ models, we take the couplings  $g_{ij}^{q,\ell}$  to be real, and assume that the  $VB$  couplings to the first-generation leptons and down-type quarks are negligible. In the quark sector, there are then three independent couplings:  $g_{ss}$ ,  $g_{sb} = g_{bs}$  and  $g_{bb}$ . Similarly, in the lepton sector, the three independent couplings are  $g_{\mu\mu}$ ,  $g_{\mu\tau} = g_{\tau\mu}$  and  $g_{\tau\tau}$ . For the leptons, these couplings hold for either component of the  $SU(2)_L$  doublet. Thus, for example,  $g_{\mu\mu} = g_{\nu_\mu\nu_\mu} = g_{\mu\nu_\mu}$ . The quark sector is a bit more complicated because the couplings to the up-type quarks involve the CKM matrix [Eq. (2)]. For example, for the  $W'$ , this implies  $g_{cb} = V_{cs}g_{sb} + V_{cb}g_{bb}$ , while for the  $Z'$ , we have  $g_{cc} = V_{cs}^2g_{ss} + 2V_{cs}V_{cb}g_{sb} + V_{cb}^2g_{bb}$ , etc. The goal of our analysis is to determine the allowed ranges of the six independent couplings.

#### IV.1. Additional observables

In addition to  $2q2\ell$  operators,  $VB$  exchange also produces four-quark ( $4q$ ) and four-lepton ( $4\ell$ ) operators at tree level. In the mass basis, the corresponding effective Lagrangian is

$$\begin{aligned} \mathcal{L}_{NP}^{4q,4\ell} = & -\frac{g_{ij}^q g_{kl}^q}{2M_V^2} (\bar{Q}_{iL}\gamma^\mu\sigma^I Q_{jL}) (\bar{Q}_{kL}\gamma_\mu\sigma^I Q_{lL}) \\ & -\frac{g_{ij}^\ell g_{kl}^\ell}{2M_V^2} (\bar{L}_{iL}\gamma^\mu\sigma^I L_{jL}) (\bar{L}_{kL}\gamma_\mu\sigma^I L_{lL}) . \end{aligned} \quad (18)$$

These contribute to five observables that yield important constraints on the  $VB$  model:  $B_s^0$ - $\bar{B}_s^0$  mixing, neutrino trident production,  $\tau \rightarrow 3\mu$ ,  $\tau \rightarrow \mu\nu\bar{\nu}$  and  $D^0$ - $\bar{D}^0$  mixing. The first three have been discussed in detail in Refs. [39, 69], the fourth in Refs. [28, 50]. The consideration of  $D^0$ - $\bar{D}^0$  mixing is new. Below we summarize the constraints.

##### IV.1.1. $B_s^0$ - $\bar{B}_s^0$ mixing

The SM contribution to  $B_s^0$ - $\bar{B}_s^0$  mixing is generated via a box diagram, and is given by

$$NC_{VLL}^{\text{SM}} (\bar{s}_L\gamma^\mu b_L) (\bar{s}_L\gamma_\mu b_L) . \quad (19)$$

The operators of Eq. (18) include

$$\frac{g_{sb}^2}{2M_V^2} (\bar{s}_L \gamma^\mu b_L) (\bar{s}_L \gamma_\mu b_L) , \quad (20)$$

which generates a contribution to  $B_s^0$ - $\bar{B}_s^0$  mixing.

Combining the SM and  $VB$  contributions, we define

$$NC_{VLL} \equiv NC_{VLL}^{\text{SM}} + \frac{g_{sb}^2}{2M_V^2} , \quad (21)$$

leading to

$$\Delta M_s = \frac{2}{3} m_{B_s} f_{B_s}^2 \hat{B}_{B_s} |NC_{VLL}| . \quad (22)$$

Taking  $f_{B_s} \sqrt{\hat{B}_{B_s}} = (266 \pm 18)$  MeV [86], the SM prediction is

$$\Delta M_s^{\text{SM}} = (17.4 \pm 2.6) \text{ ps}^{-1} . \quad (23)$$

This is to be compared with the experimental measurement [77]

$$\Delta M_s = (17.757 \pm 0.021) \text{ ps}^{-1} . \quad (24)$$

Treating the theoretical error as gaussian, this can be turned into a constraint on  $g_{sb}$  to be used in the fits:

$$\frac{g_{sb}}{M_V} = \pm (1.0_{-3.9}^{+2.0}) \times 10^{-3} \text{ TeV}^{-1} . \quad (25)$$

As was noted in Sec. III.2.3, there are more recent calculations of the hadronic parameters, and this is problematic for NP solutions of the  $b \rightarrow s \mu^+ \mu^-$  anomalies, particularly the  $Z'$  [88]. However, these new values for the hadronic parameters also cause problems for the SM itself, and so, as was done in the case of the  $U_1$  LQ model, we will await verification of this new result before including it among the constraints.

#### IV.1.2. Neutrino trident production

Neutrino trident production is the production of  $\mu^+ \mu^-$  pairs in neutrino-nucleus scattering,  $\nu_\mu N \rightarrow \nu_\mu N \mu^+ \mu^-$ . The  $Z'$  contributes to this process. Including both the SM and NP contributions, the theoretical prediction for the cross section is [69]

$$\left. \frac{\sigma_{\text{SM+NP}}}{\sigma_{\text{SM}}} \right|_{\nu N \rightarrow \nu N \mu^+ \mu^-} = \frac{1}{1 + (1 + 4s_W^2)^2} \left[ \left( 1 + \frac{v^2 g_{\mu\mu}^2}{M_V^2} \right)^2 + \left( 1 + 4s_W^2 + \frac{v^2 g_{\mu\mu}^2}{M_V^2} \right)^2 \right] . \quad (26)$$

By comparing this with the experimental measurement [78]

$$\left. \frac{\sigma_{\text{exp.}}}{\sigma_{\text{SM}}} \right|_{\nu N \rightarrow \nu N \mu^+ \mu^-} = 0.82 \pm 0.28 , \quad (27)$$

one obtains the following constraint on  $g_{\mu\mu}$  to be used in the fits:

$$\frac{g_{\mu\mu}}{M_V} = 0 \pm 1.13 \text{ TeV}^{-1} . \quad (28)$$

#### IV.1.3. $\tau \rightarrow 3\mu$

The Lagrangian of Eq. (18) includes the operator

$$- \frac{g_{\mu\mu} g_{\mu\tau}}{2M_V^2} (\bar{\mu}_L \gamma^\mu \tau_L) (\bar{\mu}_L \gamma_\mu \mu_L) , \quad (29)$$

which generates the LFV decay  $\tau \rightarrow 3\mu$ . Its decay rate is given by

$$\mathcal{B}(\tau^- \rightarrow \mu^- \mu^+ \mu^-) = X \frac{(g_{\mu\mu} g_{\mu\tau})^2}{16M_V^4} \frac{m_\tau^5 \tau_\tau}{192\pi^3}, \quad (30)$$

where  $X \approx 0.94$  is a suppression factor due to the non-zero muon mass [39].

At present, the experimental upper bound on the branching ratio for this process is [79]:

$$\mathcal{B}(\tau^- \rightarrow \mu^- \mu^+ \mu^-) < 2.1 \times 10^{-8} \text{ at } 90\% \text{ C.L.} \quad (31)$$

This leads to

$$\frac{|g_{\mu\mu} g_{\mu\tau}|}{M_V^2} < 0.013 \text{ TeV}^{-2}. \quad (32)$$

As we will see, when combined with the constraints from the  $B$  anomalies and  $B_s^0$ - $\bar{B}_s^0$  mixing, this puts an important bound on  $|g_{\mu\tau}/g_{\mu\mu}|$ .

#### IV.1.4. $\tau \rightarrow \mu\nu\bar{\nu}$

The Lagrangian of Eq. (18) also includes the operator

$$-\frac{1}{M_V^2} (-g_{\mu\tau} g_{ij} + 2g_{\mu j} g_{i\tau}) (\bar{\mu}_L \gamma^\mu \tau_L) (\bar{\nu}_{iL} \gamma_\mu \nu_{jL}), \quad (33)$$

which generates the decay  $\tau \rightarrow \mu\nu\bar{\nu}$ . The first term in the coefficient is due to the tree-level exchange of a  $Z'$ , while the second arises from  $W'$  exchange. The SM also contributes to this decay, but only for  $i = \tau$  and  $j = \mu$ . The decay rate is then proportional to

$$\left| 1 + \frac{1}{2\sqrt{2}G_F M_V^2} (-g_{\mu\tau}^2 + 2g_{\mu\mu} g_{\tau\tau}) \right|^2 + \sum'_{ij=\mu,\tau} \left| \frac{1}{2\sqrt{2}G_F M_V^2} (-g_{\mu\tau} g_{ij} + 2g_{\mu j} g_{i\tau}) \right|^2, \quad (34)$$

where the  $\sum'_{ij=\mu,\tau}$  excludes  $(i, j) = (\tau, \mu)$ .

The most stringent constraint arises from an LFUV ratio of BRs. However, a complication arises because there are two such ratios –  $\mathcal{B}(\tau \rightarrow \mu\nu\bar{\nu}/\mu \rightarrow e\nu\bar{\nu})$  and  $\mathcal{B}(\tau \rightarrow \mu\nu\bar{\nu}/\tau \rightarrow e\nu\bar{\nu})$  – and their measurements are not in complete agreement with one another [80]:

$$R_\tau^{\tau/e} \equiv \frac{\mathcal{B}(\tau \rightarrow \mu\nu\bar{\nu})/\mathcal{B}(\tau \rightarrow \mu\nu\bar{\nu})_{SM}}{\mathcal{B}(\mu \rightarrow e\nu\bar{\nu})/\mathcal{B}(\mu \rightarrow e\nu\bar{\nu})_{SM}} = 1.0060 \pm 0.0030, \quad (35)$$

$$R_\tau^{\mu/e} \equiv \frac{\mathcal{B}(\tau \rightarrow \mu\nu\bar{\nu})}{\xi_{ps} \mathcal{B}(\tau \rightarrow e\nu\bar{\nu})} = 1.0036 \pm 0.0028, \quad (36)$$

where  $\xi_{ps} = 0.9726$  is the phase-space factor. The first measurement disagrees with the SM by  $2\sigma$ , while for the second measurement, the disagreement is only at the level of  $1.3\sigma$ . Both of these apply to the quantity in Eq. (34), and we include both constraints in the fits.

As we will see,  $g_{\mu\tau}$  is quite small in the  $VB$  model. If it is neglected in Eq. (34), one obtains the constraint

$$\frac{|g_{\mu\mu} g_{\tau\tau}|}{M_V^2} = \begin{cases} 0.049 \pm 0.025 \text{ TeV}^{-2}, & R_\tau^{\tau/e} \\ 0.030 \pm 0.023 \text{ TeV}^{-2}, & R_\tau^{\mu/e} \end{cases} \quad (37)$$

Conservatively, this gives  $|g_{\mu\mu} g_{\tau\tau}|/M_V^2 < 0.1 \text{ TeV}^{-2}$ .

#### IV.1.5. $D^0$ - $\bar{D}^0$ mixing

$D^0$ - $\bar{D}^0$  mixing has been measured experimentally. It is found that [81]

$$\Delta M_D = (0.95_{-0.44}^{+0.41}) \times 10^{-2} \text{ ps}^{-1}. \quad (38)$$

Within the SM there are two types of contributions to  $D^0\text{-}\bar{D}^0$  mixing. The short-distance contributions, governed by the quark-level box diagrams, yield  $\Delta M_D = O(10^{-4}) \text{ ps}^{-1}$  [82], too small to explain the data. The long-distance contribution, from hadron exchange, is estimated to be  $\Delta M_D = (1\text{--}46) \times 10^{-3} \text{ ps}^{-1}$  [82]. Thus, it can account for the measured value of  $\Delta M_D$ , though the estimate is very uncertain.

We therefore see that  $\Delta M_D$  receives both short- and long-distance contributions, but the latter are difficult to compute with any precision. Thus, constraints on any NP contributions should really focus on the short-distance effects. In Ref. [83], all available data have been combined to extract the fundamental quantities  $|M_{12}|$  and  $|\Gamma_{12}|$ . Their fit yields

$$|M_{12}|^{\text{data}} = (6.9 \pm 2.4) \times 10^{-3} \text{ ps}^{-1} \quad , \quad |\Gamma_{12}|^{\text{data}} = (17.2 \pm 2.5) \times 10^{-3} \text{ ps}^{-1} . \quad (39)$$

$|M_{12}|^{\text{data}}$  will be used to constrain the NP.

In the  $VB$  model, there is a contribution to  $D^0\text{-}\bar{D}^0$  mixing from the tree-level exchange of the  $Z'$ . We have

$$H_{\text{eff}}^{Z'} = \frac{(g_{uc})^2}{2M_V^2} (\bar{c}_L \gamma_\mu u_L) (\bar{c}_L \gamma^\mu u_L) , \quad (40)$$

where  $g_{uc}$  is the  $\bar{c}_L u_L Z'$  coupling. This leads to

$$|M_{12}|^{Z'} = \frac{1}{3} m_D f_D^2 \hat{B}_D \left| \frac{(g_{uc})^2}{2M_V^2} \right|^2 . \quad (41)$$

To be conservative, we require only that  $|M_{12}|^{Z'}$  be less than the experimental measurement of Eq. (39). Taking  $f_D = (212.15 \pm 1.45) \text{ MeV}$  and  $\hat{B}_D = 0.75 \pm 0.03$  [86], this leads to

$$|g_{uc}| \leq 6.6 \times 10^{-4} (M_V/1 \text{ TeV}) . \quad (42)$$

Now,

$$\begin{aligned} g_{uc} &= V_{cb} V_{ub}^* g_{bb} + (V_{cs} V_{ub}^* + V_{cb} V_{us}^*) g_{sb} + V_{cs} V_{us}^* g_{ss} \\ &\simeq (0.5 + 1.3i) \times 10^{-4} g_{bb} + (1.0 + 0.3i) \times 10^{-2} g_{sb} + 0.22 g_{ss} . \end{aligned} \quad (43)$$

(Note that, although  $g_{bb}$ ,  $g_{sb}$  and  $g_{ss}$  are real,  $g_{uc}$  is complex due to the CKM matrix elements.) Applying the constraint of Eq. (42) to each of the terms individually, we find

$$|g_{bb}| \leq 4.7 (M_V/1 \text{ TeV}) \quad , \quad |g_{sb}| \leq 6.3 \times 10^{-2} (M_V/1 \text{ TeV}) \quad , \quad |g_{ss}| \leq 3 \times 10^{-3} (M_V/1 \text{ TeV}) . \quad (44)$$

Now, for  $M_V = 1 \text{ TeV}$ ,  $|g_{bb}| \leq 1$  has been imposed for perturbativity, and  $|g_{sb}| \leq O(10^{-3})$  [Eq. (25)], so the above bounds are irrelevant for these couplings. However, the bound on  $|g_{ss}|$  is important since it is the only constraint on this coupling.

## IV.2. Fits

The  $VB$  model contributes at tree level to a large number of observables, resulting in 15 constraints that must be included in the fit (we do not consider the RGE constraints). They are found in Table I ( $2q2\ell$  observables, 11 constraints), Eq. (25) ( $4q$ , 1) and Eqs. (28) and (37) ( $4\ell$ , 3). In addition, the condition of Eq. (32) must be taken into account. We now perform a fit in which the 6 couplings are the unknown parameters to be determined.

Before presenting the results of the fit, it is a very useful exercise to deduce the general pattern of the values of the couplings (throughout,  $M_V = 1 \text{ TeV}$  is assumed):

1. The constraint from  $B_s^0\text{-}\bar{B}_s^0$  mixing requires  $|g_{sb}| \lesssim O(10^{-3})$  [Eq. (25)].
2.  $C_9 = -C_{10}$  is proportional to  $g_{sb} g_{\mu\mu}$ . The constraint from the  $b \rightarrow s \mu\mu$  data leads to  $g_{sb} g_{\mu\mu} = -0.0011 \pm 0.0002$ . Since  $|g_{sb}| \lesssim O(10^{-3})$ , this then implies that  $g_{\mu\mu} \lesssim O(1)$ .
3. The constraint from  $\tau \rightarrow 3\mu$  [Eq. (32)] requires  $|g_{\mu\mu} g_{\mu\tau}| < 0.013$ . Given that  $g_{\mu\mu} \lesssim O(1)$ , this implies that  $|g_{\mu\tau}/g_{\mu\mu}| \ll 1$ .
4. Since  $g_{\mu\tau}$  is very small, the constraint of Eq. (37) applies. And since  $g_{\mu\mu} \lesssim O(1)$ , this leads to  $|g_{\tau\tau}|$  in the range 0.01–0.1.



5.  $C_V$  is proportional to  $(V_{cs} g_{sb} + V_{cb} g_{bb}) g_{\tau\tau}$ . The constraint from the  $R_{D^{(*)}}$  anomaly implies that  $(V_{cs} g_{sb} + V_{cb} g_{bb}) g_{\tau\tau} = 0.07 \pm 0.02$ . Since  $|g_{sb}| \lesssim O(10^{-3})$ , the first term is negligible, so that the  $V_{cb} g_{bb} g_{\tau\tau}$  term dominates. (This is opposite to the  $U_1$  LQ, where the first term dominated.)
6.  $C_L$  is proportional to  $g_{sb}(g_{\mu\mu} + g_{\tau\tau})$ . In order to evade the constraint from  $B \rightarrow K^{(*)} \nu \bar{\nu}$ , we require  $-0.014 \leq g_{sb}(g_{\mu\mu} + g_{\tau\tau}) \leq 0.034$ . However, because  $|g_{sb}| \lesssim O(10^{-3})$ , this is always satisfied, so there are no additional constraints on the couplings from this process.
7. Above we found  $|g_{\mu\tau}/g_{\mu\mu}| \ll 1$ . For such small values of  $g_{\mu\tau}$ , there are no constraints from the semileptonic LFV decays.
8. The only constraint on  $g_{ss}$  is in Eq. (44):  $|g_{ss}| \leq 3 \times 10^{-3}$ .

The key point is #5 above. Recall that  $R_{D^{(*)}}^{\tau/\ell} = \mathcal{B}(B^- \rightarrow D^{(*)} \tau^- \bar{\nu}_\tau) / \mathcal{B}(B^- \rightarrow D^{(*)} \ell^- \bar{\nu}_\ell)$   $\ell = e, \mu$ . Assuming that the NP affects mainly  $B^- \rightarrow D^{(*)} \tau^- \bar{\nu}_\tau$ , in order to reproduce the measured values of  $R_{D^{(*)}}$ , we require both  $g_{bb}$  and  $g_{\tau\tau}$  to be large,  $O(1)$ . However, from #4, we see that  $g_{\tau\tau}$  is constrained to be quite a bit smaller. In light of this, the NP contribution to the  $b \rightarrow c \tau^- \bar{\nu}$  amplitude is also small. The only way to generate an enhancement of  $R_{D^{(*)}}$  is if the amplitudes in the denominator are suppressed. Now, the NP can affect only  $B^- \rightarrow D^{(*)} \mu^- \bar{\nu}_\mu$ , with a contribution proportional to  $V_{cb} g_{bb} g_{\mu\mu}$ . Since both  $g_{bb}$  and  $g_{\mu\mu}$  are  $O(1)$ , this contribution can be important, leading to a suppression only if  $g_{bb} g_{\mu\mu} < 0$ . On the other hand, if such an effect were present, it would lead to a large value of  $R_{D^{(*)}}^{e/\mu} / (R_{D^{(*)}}^{e/\mu})_{\text{SM}}$ , and this is not observed (see Table I). This constraint limits the size of the NP contribution to  $B^- \rightarrow D^{(*)} \mu^- \bar{\nu}_\mu$ . The bottom line is that, while this general  $VB$  model can lead to an enhancement of  $R_{D^{(*)}}$  over its SM values, it cannot reproduce the measured central values of  $R_{D^{(*)}}$ . This will necessarily increase the  $\chi^2$  of the fit.

After performing the fit, we find  $\chi_{\text{min, SM+VB}}^2 = 15$ . Since the d.o.f. is 10 (15 constraints, 5 independent couplings, since we have only a single constraint on  $g_{ss}$ ), this gives  $\chi_{\text{min}}^2 / \text{d.o.f.} = 1.5$ , which is a marginal fit. But we understand where the problem lies: the  $VB$  model cannot explain the measured central values of  $R_{D^{(*)}}$ . In fact, the typical value of  $R_{D^{(*)}}$  that is generated in this model is roughly  $2\sigma$  below the measured values. As such, the observables  $R_{D^{(*)}}^{\tau/\ell} / (R_{D^{(*)}}^{\tau/\ell})_{\text{SM}}$  and  $R_{D^{(*)}}^{\tau/\ell} / (R_{D^{(*)}}^{\tau/\ell})_{\text{SM}}$  contribute  $\chi^2 \sim 8$  by themselves to  $\chi_{\text{min, SM+VB}}^2$ .

Even so, we do not feel that this  $VB$  model should be discarded. After all, it *can* simultaneously explain anomalies in  $b \rightarrow s \mu^+ \mu^-$  and  $b \rightarrow c \tau^- \bar{\nu}$  transitions. Obviously, if future measurements of  $R_{D^{(*)}}$  confirm the present size of the discrepancy with the SM, the  $VB$  model will be excluded. However, if it turns out that the central values of  $R_{D^{(*)}}$  are reduced, the  $VB$  model will be as viable an explanation as the  $U_1$  LQ model. For this reason, in what follows we refer to this  $VB$  model as semi-viable.

The best-fit values of the couplings are

$$\begin{aligned} g_{\mu\mu} &= -0.95_{-0.72}^{+0.42}, & g_{\mu\tau} &= 0.0 \pm 0.018, & g_{\tau\tau} &= -0.039_{-0.037}^{+0.019}, \\ g_{bb} &= 0.85_{-0.41}^{+0.96}, & g_{sb} &= (1.1_{-0.2}^{+0.9}) \times 10^{-3}, & |g_{ss}| &\leq 3 \times 10^{-3}, \end{aligned} \quad (45)$$

for  $M_V = 1$  TeV. We have several observations. First, as was the case with the  $U_1$  LQ model (Sec. III.2.1), the couplings are very poorly determined in the fit. This is again because the observables depend almost exclusively on products of the couplings, and so yield only imprecise information about the individual couplings. Even so, these values and errors indicate the size of the couplings, and these agree with our rough estimates above.

Second, we note that  $g_{\mu\tau}$  is quite small. Indeed, after performing a scan over the parameter space, we find that  $|g_{\mu\tau}/g_{\mu\mu}| \leq 0.1$  (95% C.L.). Now, the two previous analyses [39, 50] made the assumption that the NP couples predominantly to the third generation. The couplings involving the second generation obey a hierarchy  $|c_{22}| < |c_{23}|, |c_{32}| < |c_{33}|$ , where the indices indicate the generations. To be specific, these analyses have  $|g_{\mu\tau}/g_{\mu\mu}| > 1$ . But this is in clear disagreement with the data, so that the  $VB$  model is excluded as an explanation of the  $b \rightarrow s \mu^+ \mu^-$  and  $b \rightarrow c \tau^- \bar{\nu}$  anomalies. On the other hand, as we have seen above, the general  $VB$  model *is* semi-viable. We therefore conclude that its exclusion by the previous analyses is directly due to their theoretical assumption about the NP couplings.

In the interest of accuracy, it must be said that this was not the argument used by previous analyses to exclude the  $VB$  model. For example, in Ref. [50], the breaking of the  $U(2)_q \times U(2)_\ell$  flavour symmetry led naturally to values of  $O(0.1)$  for  $g_{sb}$ . (This in turn implies a small value for  $g_{\mu\mu}$ . With  $g_{\mu\tau} \simeq 0.1$  and  $g_{\mu\mu} \simeq 0.01$ , the authors found that the constraint from  $\tau \rightarrow 3\mu$  was satisfied [we agree, see Eq. (32)].) Of course, such large values of  $g_{sb}$  are in conflict with the constraints from  $B_s^0 - \bar{B}_s^0$  mixing [Eq. (25)]. However, Ref. [50] focused on the  $2q2\ell$  observables, and found that the  $B \rightarrow K^{(*)} \nu \bar{\nu}$  and RGE constraints ruled out the  $VB$  model.

Above, we found values for the couplings of the general  $VB$  model that render it semi-viable. We would like to understand the origin of this pattern of couplings. As we have seen,  $g_{\mu\tau}$  is predicted to be very small. Ideally, we would like a small value of  $g_{\mu\tau}$  to be the result of a symmetry. Now, it is often asserted that, if a model violates lepton

flavour universality, it will also lead to lepton flavour violation<sup>5</sup>. However, this is not necessarily true. In Ref. [27], it is pointed out that it is possible to construct models that violate LFU, but do not lead to sizeable LFV. This occurs when Minimal Flavour Violation [94–98] is used to construct the model. Perhaps this  $VB$  model is of this type.

### IV.3. LHC Constraints

ATLAS and CMS have examined  $pp$  collisions at  $\sqrt{s} = 13$  TeV and searched for high-mass resonances decaying into lepton pairs [99, 100]. In the  $VB$  model, it is a reasonable approximation to consider only the  $Z'$  couplings to  $b\bar{b}$  and  $\mu^+\mu^-$  [see Eq. (45)]. In this case, the relevant process is  $b\bar{b} \rightarrow Z' \rightarrow \mu^+\mu^-$ . Using this process, and assuming  $M_{Z'} = 1$  TeV, the non-observation of resonances at the LHC puts the following constraint on the couplings:

$$\frac{1.1 g_{bb}^2 g_{\mu\mu}^2}{6.0 g_{bb}^2 + 2 g_{\mu\mu}^2} \leq 3.1 \times 10^{-3} \quad (95\% \text{ C.L.}) \quad (46)$$

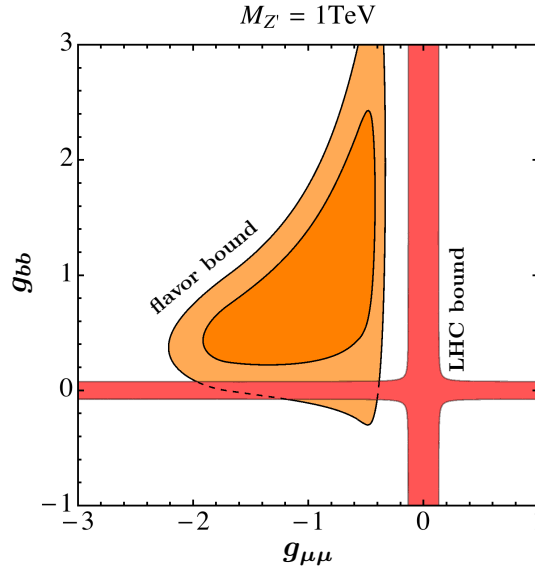


FIG. 6. Allowed regions in  $(g_{bb}, g_{\mu\mu})$  space from flavour and LHC constraints, assuming  $M_{Z'} = 1$  TeV. The  $1\sigma$  and  $2\sigma$  flavour bounds are shown respectively in the dark and light orange regions. The 95% C.L. LHC bound is shown in the red region.

In Fig. 6 we show the allowed regions in  $(g_{bb}, g_{\mu\mu})$  space from the flavour and LHC constraints. At  $1\sigma$  in the flavour constraints, the regions do not overlap. However, the  $2\sigma$  region does overlap, suggesting that the  $VB$  model might be viable. In order to quantify this, we include the LHC result in the fit by converting the 95% C.L. upper limit (UL) of Eq. (47) to a bound of  $0 \pm \text{UL}/2$ :

$$\frac{1.1 g_{bb}^2 g_{\mu\mu}^2}{6.0 g_{bb}^2 + 2 g_{\mu\mu}^2} = 0.0 \pm 1.55 \times 10^{-3} . \quad (47)$$

Now we find  $\chi_{min, \text{SM}+VB}^2 = 19.3$ . The d.o.f. is 11 (16 constraints, 5 independent couplings), so that  $\chi_{min}^2/\text{d.o.f.} = 1.8$ , which is a poor fit.

We are forced to conclude that, in the end, the  $VB$  model is excluded as a possible combined explanation of the  $b \rightarrow s\mu^+\mu^-$  and  $b \rightarrow c\tau^-\bar{\nu}$  anomalies. We stress that this conclusion is independent of any assumption about the NP couplings. It is found simply by taking into account all the flavour constraints and the bound from the LHC dimuon search.

There is one possible loophole. If the  $Z'$  has additional, invisible decays, perhaps to dark matter [101], the LHC constraints can be evaded. In this case, the  $VB$  model would still be permitted.

<sup>5</sup> This was the main point of Ref. [93]. To illustrate this, the scenario of NP that couples only to the third generation in the weak basis was used.

## V. CONCLUSIONS

At the present time, there are a number of measurements that are in disagreement with the predictions of the SM. The observables all involve the quark-level transitions  $b \rightarrow s\mu^+\mu^-$  or  $b \rightarrow c\tau^-\bar{\nu}$ . It was shown that, theoretically, both anomalies could be explained within the same new-physics model, and four possibilities were identified. There are three leptoquark models –  $S_3$ ,  $U_3$ ,  $U_1$  – and the  $VB$  model, containing SM-like  $W'$  and  $Z'$  vector bosons. These four NP models were examined in recent analyses, under the theoretical assumption that the NP couples predominantly to the third generation, with the couplings involving the second generation subdominant. It was found that, when constraints from other processes are taken into account, the  $S_3$ ,  $U_3$  and  $VB$  models cannot explain the  $B$  anomalies, but  $U_1$  is viable. However, this raises the question: to what extent do these conclusions depend on the theoretical assumption regarding the NP couplings? In this paper, we reanalyze the models, but without any assumption about their couplings.

In LQ models, there are new tree-level contributions to semileptonic processes involving two quarks and two leptons. Now, several of the  $B$  anomalies violate lepton flavour universality, suggesting that any NP explanations may also lead to lepton-flavour-violating effects. And indeed, there are several  $2q2\ell$  LFV processes:  $B \rightarrow K^{(*)}\mu^\pm\tau^\mp$ ,  $\tau \rightarrow \mu\phi$ ,  $\Upsilon \rightarrow \mu\tau$  and  $J/\psi \rightarrow \mu\tau$ . However, these were not fully taken into account in previous analyses. We find that constraints from these processes are extremely important.

For the LQ models, we show that, even if the LFV constraints are not applied,  $S_3$  and  $U_3$  cannot explain the  $B$ -decay anomalies. On the other hand,  $U_1$  is a viable model. The problem is that, while products of the LQ couplings are found to lie in certain ranges of values, there is very little information about the individual couplings themselves. This is greatly improved when the LFV constraints are added. We find that the region of allowed couplings is greatly reduced, and is similar (though somewhat larger) to that found when the NP couples predominantly to the third generation. That is, the experimental data suggest a pattern of LQ couplings similar to that of the theoretical assumption.

The LFV constraints have an additional effect. The scale of NP is well above the weak scale. When the NP is integrated out, this produces  $\mathcal{L}_{\text{NP}}$ , which contains effective four-fermion operators. It is assumed that these are dominated by the  $2q2\ell$  operators that contribute to  $b \rightarrow s\mu^+\mu^-$  or  $b \rightarrow c\tau^-\bar{\nu}$ . When the full Lagrangian,  $\mathcal{L}_{\text{SM}} + \mathcal{L}_{\text{NP}}$ , is evolved to low energies using the renormalization group equations, this produces new operators and corrections to SM operators. It has been argued that all of these effects lead to additional, important constraints on the NP, and reduce the region of allowed couplings. In this paper, we point out that these constraints are not rigorous. In real models,  $\mathcal{L}_{\text{NP}}$  may contain additional operators, both dominant and subdominant, that can change the conclusions of the RGE analysis. But even if one accepts the RGE constraints, we show that, if one requires  $|h_{ij}| \leq 1$  (so that the couplings remain perturbative), the LFV constraints, which were ignored in the RGE discussion, lead to a much larger reduction of the allowed region of NP couplings. That is, the RGE constraints are unimportant.

The  $U_1$  LQ model is therefore a viable candidate for simultaneously explaining the  $b \rightarrow s\mu^+\mu^-$  or  $b \rightarrow c\tau^-\bar{\nu}$  anomalies. If correct, observable effects in other processes are predicted. In particular, the violation of lepton flavour universality in  $B \rightarrow \pi\ell\bar{\nu}_\ell$  or  $B^- \rightarrow \ell\bar{\nu}_\ell$  decays may be enhanced over the SM by as much as 40%.  $\mathcal{B}(B \rightarrow K^{(*)}\nu\bar{\nu})$  may be increased by 70% over the SM. And  $\mathcal{B}(B \rightarrow K^{(*)}\tau^+\tau^-)$  and  $\mathcal{B}(B_s^0 \rightarrow \tau^+\tau^-)$  may be enhanced by as much as three orders of magnitude. Most importantly, these predictions are correlated with one another, and with the value of  $R_{D^{*\ell}}^\tau/(R_{D^{*\ell}}^\tau)_{\text{SM}}$ . This is a good test of the  $U_1$  model.

For the  $VB$  model, the conclusions are quite different than for the LQ models. First, there are also tree-level contributions to four-quark and four-lepton observables, and these lead to important additional constraints on the couplings (values are given assuming  $M_V = 1$  TeV). In particular, the constraint from  $B_s^0$ - $\bar{B}_s^0$  mixing implies that  $|g_{sb}| \lesssim O(10^{-3})$ . In turn, in order to explain the  $b \rightarrow s\mu^+\mu^-$  anomaly,  $g_{\mu\mu} \lesssim O(1)$  is required. Finally, in order to evade the constraint from  $\tau \rightarrow 3\mu$ ,  $g_{\mu\tau}$  must be sufficiently small. We find that, when all constraints are applied to the  $VB$  model,  $|g_{\mu\tau}/g_{\mu\mu}| < 0.1$  is required. If the NP couples predominantly to the third generation, it is found that the  $Z'$  couplings involving the second-generation leptons obey  $|g_{\mu\tau}| > |g_{\mu\mu}|$ . This clearly rules out the  $VB$  model with the above theoretical assumption about its couplings. (Previous analyses also ruled out the  $VB$  model, but for other reasons.)

Another process to which  $VB$  contributes at tree level is  $\tau \rightarrow \mu\nu\bar{\nu}$ , and the constraints are very stringent. Given that  $g_{\mu\mu} \lesssim O(1)$ , they lead to a value for  $|g_{\tau\tau}|$  in the range 0.01-0.1. The NP contribution to  $B^- \rightarrow D^{(*)}\tau^-\bar{\nu}_\tau$  is proportional to  $g_{bb}g_{\tau\tau}$ . Even though  $g_{bb} = O(1)$ , such a small value of  $|g_{\tau\tau}|$  leads to a small NP effect, and makes it impossible to reproduce the measured central values of  $R_{D^{(*)}}$ . There is an enhancement of  $R_{D^{(*)}}$  (due to a suppression of  $B^- \rightarrow D^{(*)}\mu^-\bar{\nu}_\mu$ ), but it is smaller than what is observed. Thus, the  $VB$  model would be viable only if future measurements find that the central values of  $R_{D^{(*)}}$  are reduced.

Now, the process  $b\bar{b} \rightarrow Z' \rightarrow \mu^+\mu^-$  leads to the production of high-mass resonant dimuon pairs in  $pp$  collisions at  $\sqrt{s} = 13$  TeV. Unfortunately, since both  $g_{bb}$  and  $g_{\mu\mu}$  are  $\lesssim O(1)$ , this leads to a production rate larger than the limits placed by ATLAS and CMS. The only way to evade this is if the  $Z'$  has additional, invisible decays. If this

does not occur, the upshot is that, in the end, the  $VB$  model is excluded as a possible combined explanation of the  $B$  anomalies. However, this conclusion is not the result of any assumption about the NP couplings. Rather, it is found simply by taking into account all the flavour constraints and the bound from the LHC dimuon search.

**Acknowledgments:** JK would like to thank David Straub and Michael Paraskevas for very useful discussions. This work was financially supported by NSERC of Canada (DL, RW).

- 
- [1] R. Aaij *et al.* [LHCb Collaboration], “Measurement of Form-Factor-Independent Observables in the Decay  $B^0 \rightarrow K^{*0}\mu^+\mu^-$ ,” *Phys. Rev. Lett.* **111**, 191801 (2013) doi:10.1103/PhysRevLett.111.191801 [arXiv:1308.1707 [hep-ex]].
  - [2] R. Aaij *et al.* [LHCb Collaboration], “Angular analysis of the  $B^0 \rightarrow K^{*0}\mu^+\mu^-$  decay using  $3\text{ fb}^{-1}$  of integrated luminosity,” *JHEP* **1602**, 104 (2016) doi:10.1007/JHEP02(2016)104 [arXiv:1512.04442 [hep-ex]].
  - [3] A. Abdesselam *et al.* [Belle Collaboration], “Angular analysis of  $B^0 \rightarrow K^*(892)^0\ell^+\ell^-$ ,” arXiv:1604.04042 [hep-ex].
  - [4] ATLAS Collaboration, “Angular analysis of  $B_d^0 \rightarrow K^*\mu^+\mu^-$  decays in  $pp$  collisions at  $\sqrt{s} = 8\text{ TeV}$  with the ATLAS detector,” Tech. Rep. ATLAS-CONF-2017-023, CERN, Geneva, 2017.
  - [5] CMS Collaboration, “Measurement of the  $P_1$  and  $P_5'$  angular parameters of the decay  $B^0 \rightarrow K^{*0}\mu^+\mu^-$  in proton-proton collisions at  $\sqrt{s} = 8\text{ TeV}$ ,” Tech. Rep. CMS-PAS-BPH-15-008, CERN, Geneva, 2017.
  - [6] R. Aaij *et al.* [LHCb Collaboration], “Differential branching fraction and angular analysis of the decay  $B_s^0 \rightarrow \phi\mu^+\mu^-$ ,” *JHEP* **1307**, 084 (2013) doi:10.1007/JHEP07(2013)084 [arXiv:1305.2168 [hep-ex]].
  - [7] R. Aaij *et al.* [LHCb Collaboration], “Angular analysis and differential branching fraction of the decay  $B_s^0 \rightarrow \phi\mu^+\mu^-$ ,” *JHEP* **1509**, 179 (2015) doi:10.1007/JHEP09(2015)179 [arXiv:1506.08777 [hep-ex]].
  - [8] R. Aaij *et al.* [LHCb Collaboration], “Test of lepton universality using  $B^+ \rightarrow K^+\ell^+\ell^-$  decays,” *Phys. Rev. Lett.* **113**, 151601 (2014) doi:10.1103/PhysRevLett.113.151601 [arXiv:1406.6482 [hep-ex]].
  - [9] R. Aaij *et al.* [LHCb Collaboration], “Test of lepton universality with  $B^0 \rightarrow K^{*0}\ell^+\ell^-$  decays,” *JHEP* **1708**, 055 (2017) doi:10.1007/JHEP08(2017)055 [arXiv:1705.05802 [hep-ex]].
  - [10] B. Capdevila, A. Crivellin, S. Descotes-Genon, J. Matias and J. Virto, “Patterns of New Physics in  $b \rightarrow s\ell^+\ell^-$  transitions in the light of recent data,” *JHEP* **1801**, 093 (2018) doi:10.1007/JHEP01(2018)093 [arXiv:1704.05340 [hep-ph]].
  - [11] W. Altmannshofer, P. Stangl and D. M. Straub, “Interpreting Hints for Lepton Flavor Universality Violation,” *Phys. Rev. D* **96**, no. 5, 055008 (2017) doi:10.1103/PhysRevD.96.055008 [arXiv:1704.05435 [hep-ph]].
  - [12] G. D’Amico, M. Nardecchia, P. Panci, F. Sannino, A. Strumia, R. Torre and A. Urbano, “Flavor anomalies after the  $R_{K^*}$  measurement,” *JHEP* **1709**, 010 (2017) doi:10.1007/JHEP09(2017)010 [arXiv:1704.05438 [hep-ph]].
  - [13] G. Hiller and I. Nisandzic, “ $R_K$  and  $R_{K^*}$  beyond the standard model,” *Phys. Rev. D* **96**, no. 3, 035003 (2017) doi:10.1103/PhysRevD.96.035003 [arXiv:1704.05444 [hep-ph]].
  - [14] L. S. Geng, B. Grinstein, S. Jäger, J. Martin Camalich, X. L. Ren and R. X. Shi, “Towards the discovery of new physics with lepton-universality ratios of  $b \rightarrow s\ell\ell$  decays,” *Phys. Rev. D* **96**, no. 9, 093006 (2017) doi:10.1103/PhysRevD.96.093006 [arXiv:1704.05446 [hep-ph]].
  - [15] M. Ciuchini, A. M. Coutinho, M. Fedele, E. Franco, A. Paul, L. Silvestrini and M. Valli, “On Flavorful Easter eggs for New Physics hunger and Lepton Flavor Universality violation,” *Eur. Phys. J. C* **77**, no. 10, 688 (2017) doi:10.1140/epjc/s10052-017-5270-2 [arXiv:1704.05447 [hep-ph]].
  - [16] A. Celis, J. Fuentes-Martin, A. Vicente and J. Virto, “Gauge-invariant implications of the LHCb measurements on lepton-flavor nonuniversality,” *Phys. Rev. D* **96**, no. 3, 035026 (2017) doi:10.1103/PhysRevD.96.035026 [arXiv:1704.05672 [hep-ph]].
  - [17] A. K. Alok, B. Bhattacharya, A. Datta, D. Kumar, J. Kumar and D. London, “New Physics in  $b \rightarrow s\mu^+\mu^-$  after the Measurement of  $R_{K^*}$ ,” *Phys. Rev. D* **96**, no. 9, 095009 (2017) doi:10.1103/PhysRevD.96.095009 [arXiv:1704.07397 [hep-ph]].
  - [18] J. P. Lees *et al.* [BaBar Collaboration], “Measurement of an Excess of  $\bar{B} \rightarrow D^{(*)}\tau^-\bar{\nu}_\tau$  Decays and Implications for Charged Higgs Bosons,” *Phys. Rev. D* **88**, 072012 (2013) doi:10.1103/PhysRevD.88.072012 [arXiv:1303.0571 [hep-ex]].
  - [19] M. Huschle *et al.* [Belle Collaboration], “Measurement of the branching ratio of  $\bar{B} \rightarrow D^{(*)}\tau^-\bar{\nu}_\tau$  relative to  $\bar{B} \rightarrow D^{(*)}\ell^-\bar{\nu}_\ell$  decays with hadronic tagging at Belle,” *Phys. Rev. D* **92**, 072014 (2015) doi:10.1103/PhysRevD.92.072014 [arXiv:1507.03233 [hep-ex]].
  - [20] R. Aaij *et al.* [LHCb Collaboration], “Measurement of the ratio of branching fractions  $\mathcal{B}(\bar{B}^0 \rightarrow D^{*+}\tau^-\bar{\nu}_\tau)/\mathcal{B}(\bar{B}^0 \rightarrow D^{*+}\mu^-\bar{\nu}_\mu)$ ,” *Phys. Rev. Lett.* **115**, 111803 (2015) Addendum: [Phys. Rev. Lett. **115**, 159901 (2015)] doi:10.1103/PhysRevLett.115.159901, 10.1103/PhysRevLett.115.111803 [arXiv:1506.08614 [hep-ex]].
  - [21] A. Abdesselam *et al.*, “Measurement of the  $\tau$  lepton polarization in the decay  $\bar{B} \rightarrow D^*\tau^-\bar{\nu}_\tau$ ,” arXiv:1608.06391 [hep-ex].
  - [22] R. Aaij *et al.* [LHCb Collaboration], “Measurement of the ratio of branching fractions  $\mathcal{B}(B_c^+ \rightarrow J/\psi\tau^+\nu_\tau)/\mathcal{B}(B_c^+ \rightarrow J/\psi\mu^+\nu_\mu)$ ,” *Phys. Rev. Lett.* **120**, no. 12, 121801 (2018) doi:10.1103/PhysRevLett.120.121801 [arXiv:1711.05623 [hep-ex]].
  - [23] F. U. Bernlochner, Z. Ligeti, M. Papucci and D. J. Robinson, “Combined analysis of semileptonic  $B$  decays to  $D$  and  $D^*$ :  $R(D^{(*)})$ ,  $|V_{cb}|$ , and new physics,” *Phys. Rev. D* **95**, no. 11, 115008 (2017) Erratum: [Phys. Rev. D **97**, no. 5, 059902 (2018)] doi:10.1103/PhysRevD.95.115008, 10.1103/PhysRevD.97.059902 [arXiv:1703.05330 [hep-ph]].
  - [24] D. Bigi, P. Gambino and S. Schacht, “ $R(D^*)$ ,  $|V_{cb}|$ , and the Heavy Quark Symmetry relations between form factors,” *JHEP* **1711**, 061 (2017) doi:10.1007/JHEP11(2017)061 [arXiv:1707.09509 [hep-ph]].

- [25] R. Watanabe, “New Physics effect on  $B_c \rightarrow J/\psi \tau \bar{\nu}$  in relation to the  $R_{D^{(*)}}$  anomaly,” Phys. Lett. B **776**, 5 (2018) doi:10.1016/j.physletb.2017.11.016 [arXiv:1709.08644 [hep-ph]].
- [26] B. Bhattacharya, A. Datta, D. London and S. Shivashankara, “Simultaneous Explanation of the  $R_K$  and  $R(D^{(*)})$  Puzzles,” Phys. Lett. B **742**, 370 (2015) doi:10.1016/j.physletb.2015.02.011 [arXiv:1412.7164 [hep-ph]].
- [27] R. Alonso, B. Grinstein and J. M. Camalich, “Lepton universality violation and lepton flavor conservation in  $B$ -meson decays,” JHEP **1510**, 184 (2015) doi:10.1007/JHEP10(2015)184 [arXiv:1505.05164 [hep-ph]].
- [28] A. Greljo, G. Isidori and D. Marzocca, “On the breaking of Lepton Flavor Universality in  $B$  decays,” JHEP **1507**, 142 (2015) doi:10.1007/JHEP07(2015)142 [arXiv:1506.01705 [hep-ph]].
- [29] L. Calibbi, A. Crivellin and T. Ota, “Effective Field Theory Approach to  $b \rightarrow s \ell \ell^{(\prime)}$ ,  $B \rightarrow K^{(*)} \nu \bar{\nu}$  and  $B \rightarrow D^{(*)} \tau \nu$  with Third Generation Couplings,” Phys. Rev. Lett. **115**, 181801 (2015) doi:10.1103/PhysRevLett.115.181801 [arXiv:1506.02661 [hep-ph]].
- [30] M. Bauer and M. Neubert, “Minimal Leptoquark Explanation for the  $R_{D^{(*)}}$ ,  $R_K$ , and  $(g-2)_\mu$  Anomalies,” Phys. Rev. Lett. **116**, no. 14, 141802 (2016) doi:10.1103/PhysRevLett.116.141802 [arXiv:1511.01900 [hep-ph]].
- [31] S. Fajfer and N. Košnik, “Vector leptoquark resolution of  $R_K$  and  $R_{D^{(*)}}$  puzzles,” Phys. Lett. B **755**, 270 (2016) doi:10.1016/j.physletb.2016.02.018 [arXiv:1511.06024 [hep-ph]].
- [32] R. Barbieri, G. Isidori, A. Pattori and F. Senia, “Anomalies in  $B$ -decays and  $U(2)$  flavor symmetry,” Eur. Phys. J. C **76**, no. 2, 67 (2016) doi:10.1140/epjc/s10052-016-3905-3 [arXiv:1512.01560 [hep-ph]].
- [33] S. M. Boucenna, A. Celis, J. Fuentes-Martin, A. Vicente and J. Virto, “Non-abelian gauge extensions for  $B$ -decay anomalies,” Phys. Lett. B **760**, 214 (2016) doi:10.1016/j.physletb.2016.06.067 [arXiv:1604.03088 [hep-ph]].
- [34] D. Das, C. Hati, G. Kumar and N. Mahajan, “Towards a unified explanation of  $R_{D^{(*)}}$ ,  $R_K$  and  $(g-2)_\mu$  anomalies in a left-right model with leptoquarks,” Phys. Rev. D **94**, 055034 (2016) doi:10.1103/PhysRevD.94.055034 [arXiv:1605.06313 [hep-ph]].
- [35] F. Feruglio, P. Paradisi and A. Pattori, “Revisiting Lepton Flavor Universality in  $B$  Decays,” Phys. Rev. Lett. **118**, no. 1, 011801 (2017) doi:10.1103/PhysRevLett.118.011801 [arXiv:1606.00524 [hep-ph]].
- [36] S. M. Boucenna, A. Celis, J. Fuentes-Martin, A. Vicente and J. Virto, “Phenomenology of an  $SU(2) \times SU(2) \times U(1)$  model with lepton-flavor non-universality,” JHEP **1612**, 059 (2016) doi:10.1007/JHEP12(2016)059 [arXiv:1608.01349 [hep-ph]].
- [37] D. Becirevic, S. Fajfer, N. Košnik and O. Sumensari, “Leptoquark model to explain the  $B$ -physics anomalies,  $R_K$  and  $R_D$ ,” Phys. Rev. D **94**, no. 11, 115021 (2016) doi:10.1103/PhysRevD.94.115021 [arXiv:1608.08501 [hep-ph]].
- [38] S. Sahoo, R. Mohanta and A. K. Giri, “Explaining the  $R_K$  and  $R_{D^{(*)}}$  anomalies with vector leptoquarks,” Phys. Rev. D **95**, no. 3, 035027 (2017) doi:10.1103/PhysRevD.95.035027 [arXiv:1609.04367 [hep-ph]].
- [39] B. Bhattacharya, A. Datta, J. P. Guévin, D. London and R. Watanabe, “Simultaneous Explanation of the  $R_K$  and  $R_{D^{(*)}}$  Puzzles: a Model Analysis,” JHEP **1701**, 015 (2017) doi:10.1007/JHEP01(2017)015 [arXiv:1609.09078 [hep-ph]].
- [40] R. Barbieri, C. W. Murphy and F. Senia, “ $B$ -decay Anomalies in a Composite Leptoquark Model,” Eur. Phys. J. C **77**, no. 1, 8 (2017) doi:10.1140/epjc/s10052-016-4578-7 [arXiv:1611.04930 [hep-ph]].
- [41] M. Bordone, G. Isidori and S. Trifinopoulos, “Semileptonic  $B$ -physics anomalies: A general EFT analysis within  $U(2)^n$  flavor symmetry,” Phys. Rev. D **96**, no. 1, 015038 (2017) doi:10.1103/PhysRevD.96.015038 [arXiv:1702.07238 [hep-ph]].
- [42] C. H. Chen, T. Nomura and H. Okada, “Excesses of muon  $g-2$ ,  $R_{D^{(*)}}$ , and  $R_K$  in a leptoquark model,” Phys. Lett. B **774**, 456 (2017) doi:10.1016/j.physletb.2017.10.005 [arXiv:1703.03251 [hep-ph]].
- [43] E. Megias, M. Quiros and L. Salas, “Lepton-flavor universality violation in  $R_K$  and  $R_{D^{(*)}}$  from warped space,” JHEP **1707**, 102 (2017) doi:10.1007/JHEP07(2017)102 [arXiv:1703.06019 [hep-ph]].
- [44] A. Crivellin, D. Müller and T. Ota, “Simultaneous explanation of  $R(D^{(*)})$  and  $b \rightarrow s \mu^+ \mu^-$ : the last scalar leptoquarks standing,” JHEP **1709**, 040 (2017) doi:10.1007/JHEP09(2017)040 [arXiv:1703.09226 [hep-ph]].
- [45] W. Altmannshofer, P. S. Bhupal Dev and A. Soni, “ $R_{D^{(*)}}$  anomaly: A possible hint for natural supersymmetry with  $R$ -parity violation,” Phys. Rev. D **96**, no. 9, 095010 (2017) doi:10.1103/PhysRevD.96.095010 [arXiv:1704.06659 [hep-ph]].
- [46] A. K. Alok, D. Kumar, J. Kumar and R. Sharma, “Lepton flavor non-universality in the  $B$ -sector: a global analyses of various new physics models,” arXiv:1704.07347 [hep-ph].
- [47] F. Feruglio, P. Paradisi and A. Pattori, “On the Importance of Electroweak Corrections for  $B$  Anomalies,” JHEP **1709**, 061 (2017) doi:10.1007/JHEP09(2017)061 [arXiv:1705.00929 [hep-ph]].
- [48] S. Matsuzaki, K. Nishiwaki and R. Watanabe, “Phenomenology of flavorful composite vector bosons in light of  $B$  anomalies,” JHEP **1708**, 145 (2017) doi:10.1007/JHEP08(2017)145 [arXiv:1706.01463 [hep-ph]].
- [49] I. Doršner, S. Fajfer, D. A. Faroughy and N. Košnik, “The role of the  $S_3$  GUT leptoquark in flavor universality and collider searches,” JHEP **1710**, 188 (2017) doi:10.1007/JHEP10(2017)188 [arXiv:1706.07779 [hep-ph]].
- [50] D. Buttazzo, A. Greljo, G. Isidori and D. Marzocca, “ $B$ -physics anomalies: a guide to combined explanations,” JHEP **1711**, 044 (2017) doi:10.1007/JHEP11(2017)044 [arXiv:1706.07808 [hep-ph]].
- [51] D. Choudhury, A. Kundu, R. Mandal and R. Sinha, “Minimal unified resolution to  $R_{K^{(*)}}$  and  $R(D^{(*)})$  anomalies with lepton mixing,” Phys. Rev. Lett. **119**, no. 15, 151801 (2017) doi:10.1103/PhysRevLett.119.151801 [arXiv:1706.08437 [hep-ph]].
- [52] N. Assad, B. Fornal and B. Grinstein, “Baryon Number and Lepton Universality Violation in Leptoquark and Diquark Models,” Phys. Lett. B **777**, 324 (2018) doi:10.1016/j.physletb.2017.12.042 [arXiv:1708.06350 [hep-ph]].
- [53] L. Di Luzio, A. Greljo and M. Nardecchia, “Gauge leptoquark as the origin of  $B$ -physics anomalies,” Phys. Rev. D **96**, no. 11, 115011 (2017) doi:10.1103/PhysRevD.96.115011 [arXiv:1708.08450 [hep-ph]].
- [54] L. Calibbi, A. Crivellin and T. Li, “A model of vector leptoquarks in view of the  $B$ -physics anomalies,” arXiv:1709.00692 [hep-ph].

- [55] B. Chauhan and B. Kindra, “Invoking Chiral Vector Leptoquark to explain LFU violation in  $B$  Decays,” arXiv:1709.09989 [hep-ph].
- [56] M. Bordone, C. Cornella, J. Fuentes-Martin and G. Isidori, “A three-site gauge model for flavor hierarchies and flavor anomalies,” Phys. Lett. B **779**, 317 (2018) doi:10.1016/j.physletb.2018.02.011 [arXiv:1712.01368 [hep-ph]].
- [57] D. Choudhury, A. Kundu, R. Mandal and R. Sinha, “ $R_{K^{(*)}}$  and  $R(D^{(*)})$  anomalies resolved with lepton mixing,” arXiv:1712.01593 [hep-ph].
- [58] K. Fuyuto, H. L. Li and J. H. Yu, “Implications of hidden gauged  $U(1)$  model for  $B$  anomalies,” Phys. Rev. D **97**, no. 11, 115003 (2018) doi:10.1103/PhysRevD.97.115003 [arXiv:1712.06736 [hep-ph]].
- [59] R. Barbieri and A. Tesi, “ $B$ -decay anomalies in Pati-Salam  $SU(4)$ ,” Eur. Phys. J. C **78**, no. 3, 193 (2018) doi:10.1140/epjc/s10052-018-5680-9 [arXiv:1712.06844 [hep-ph]].
- [60] G. D’Ambrosio and A. M. Iyer, “Flavour issues in warped custodial models:  $B$  anomalies and rare  $K$  decays,” Eur. Phys. J. C **78**, no. 6, 448 (2018) doi:10.1140/epjc/s10052-018-5915-9 [arXiv:1712.08122 [hep-ph]].
- [61] M. Blanke and A. Crivellin, “ $B$  Meson Anomalies in a Pati-Salam Model within the Randall-Sundrum Background,” arXiv:1801.07256 [hep-ph].
- [62] A. Azatov, D. Barducci, D. Ghosh, D. Marzocca and L. Ubaldi, “Combined explanations of  $B$ -physics anomalies: the sterile neutrino solution,” arXiv:1807.10745 [hep-ph].
- [63] J. Aebischer, A. Crivellin, M. Fael and C. Greub, “Matching of gauge invariant dimension-six operators for  $b \rightarrow s$  and  $b \rightarrow c$  transitions,” JHEP **1605**, 037 (2016) doi:10.1007/JHEP05(2016)037 [arXiv:1512.02830 [hep-ph]].
- [64] A. Dedes, W. Materkowska, M. Paraskevas, J. Rosiek and K. Suxho, “Feynman rules for the Standard Model Effective Field Theory in  $R_\xi$ -gauges,” JHEP **1706**, 143 (2017) doi:10.1007/JHEP06(2017)143 [arXiv:1704.03888 [hep-ph]].
- [65] The importance of  $\Upsilon$  and  $J/\psi$  decays for assessing proposed solutions of the  $b \rightarrow c\tau^-\bar{\nu}$  anomaly was emphasized in D. Aloni, A. Efrati, Y. Grossman and Y. Nir, “ $\Upsilon$  and  $\psi$  leptonic decays as probes of solutions to the  $R_D^{(*)}$  puzzle,” JHEP **1706**, 019 (2017) doi:10.1007/JHEP06(2017)019 [arXiv:1702.07356 [hep-ph]].
- [66] B. Chakraborty *et al.* [HPQCD Collaboration], “Nonperturbative comparison of clover and highly improved staggered quarks in lattice QCD and the properties of the  $\phi$  meson,” Phys. Rev. D **96**, no. 7, 074502 (2017) doi:10.1103/PhysRevD.96.074502 [arXiv:1703.05552 [hep-lat]].
- [67] D. Bećirević, G. Duplanić, B. Klajn, B. Melić and F. Sanfilippo, “Lattice QCD and QCD sum rule determination of the decay constants of  $\eta_c$ ,  $J/\psi$  and  $h_c$  states,” Nucl. Phys. B **883**, 306 (2014) doi:10.1016/j.nuclphysb.2014.03.024 [arXiv:1312.2858 [hep-ph]].
- [68] A. Abdesselam *et al.* [Belle Collaboration], “Precise determination of the CKM matrix element  $|V_{cb}|$  with  $\bar{B}^0 \rightarrow D^{*+} \ell^- \bar{\nu}_\ell$  decays with hadronic tagging at Belle,” arXiv:1702.01521 [hep-ex].
- [69] A. K. Alok, B. Bhattacharya, D. Kumar, J. Kumar, D. London and S. U. Sankar, “New physics in  $b \rightarrow s\mu^+\mu^-$ : Distinguishing models through CP-violating effects,” Phys. Rev. D **96**, no. 1, 015034 (2017) doi:10.1103/PhysRevD.96.015034 [arXiv:1703.09247 [hep-ph]].
- [70] J. P. Lees *et al.* [BaBar Collaboration], “A search for the decay modes  $B^{+-} \rightarrow h^{+-}\tau^+l$ ,” Phys. Rev. D **86**, 012004 (2012) doi:10.1103/PhysRevD.86.012004 [arXiv:1204.2852 [hep-ex]].
- [71] J. P. Lees *et al.* [BaBar Collaboration], “Search for Charged Lepton Flavor Violation in Narrow Upsilon Decays,” Phys. Rev. Lett. **104**, 151802 (2010) doi:10.1103/PhysRevLett.104.151802 [arXiv:1001.1883 [hep-ex]].
- [72] Y. Miyazaki *et al.* [Belle Collaboration], “Search for Lepton-Flavor-Violating tau Decays into a Lepton and a Vector Meson,” Phys. Lett. B **699**, 251 (2011) doi:10.1016/j.physletb.2011.04.011 [arXiv:1101.0755 [hep-ex]].
- [73] M. Ablikim *et al.* [BES Collaboration], “Search for the lepton flavor violation processes  $J/\psi \rightarrow \mu\tau$  and  $e\tau$ ,” Phys. Lett. B **598**, 172 (2004) doi:10.1016/j.physletb.2004.08.005 [hep-ex/0406018].
- [74] Y. Sakaki, M. Tanaka, A. Tayduganov and R. Watanabe, “Testing leptoquark models in  $\bar{B} \rightarrow D^{(*)}\tau\bar{\nu}$ ,” Phys. Rev. D **88**, 094012 (2013) doi:10.1103/PhysRevD.88.094012 [arXiv:1309.0301 [hep-ph]].
- [75] A. Crivellin, D. Mller, A. Signer and Y. Ulrich, “Correlating lepton flavor universality violation in  $B$  decays with  $\mu \rightarrow e\gamma$  using leptoquarks,” Phys. Rev. D **97**, no. 1, 015019 (2018) doi:10.1103/PhysRevD.97.015019 [arXiv:1706.08511 [hep-ph]].
- [76] C. Bobeth and A. J. Buras, “Leptoquarks meet  $\varepsilon'/\varepsilon$  and rare Kaon processes,” JHEP **1802**, 101 (2018) doi:10.1007/JHEP02(2018)101 [arXiv:1712.01295 [hep-ph]].
- [77] Y. Amhis *et al.* [HFLAV Collaboration], “Averages of  $b$ -hadron,  $c$ -hadron, and  $\tau$ -lepton properties as of summer 2016,” Eur. Phys. J. C **77**, no. 12, 895 (2017) doi:10.1140/epjc/s10052-017-5058-4 [arXiv:1612.07233 [hep-ex]].
- [78] S. R. Mishra *et al.* [CCFR Collaboration], “Neutrino tridents and  $W$ - $Z$  interference,” Phys. Rev. Lett. **66**, 3117 (1991). doi:10.1103/PhysRevLett.66.3117
- [79] K. Hayasaka *et al.*, “Search for Lepton Flavor Violating Tau Decays into Three Leptons with 719 Million Produced Tau+Tau- Pairs,” Phys. Lett. B **687**, 139 (2010) doi:10.1016/j.physletb.2010.03.037 [arXiv:1001.3221 [hep-ex]].
- [80] A. Pich, “Precision Tau Physics,” Prog. Part. Nucl. Phys. **75**, 41 (2014) doi:10.1016/j.pnpnp.2013.11.002 [arXiv:1310.7922 [hep-ph]].
- [81] M. Tanabashi *et al.* (Particle Data Group), Phys. Rev. D **98**, 030001 (2018).
- [82] V. D. Barger, J. L. Hewett and R. J. N. Phillips, “New Constraints on the Charged Higgs Sector in Two Higgs Doublet Models,” Phys. Rev. D **41**, 3421 (1990). doi:10.1103/PhysRevD.41.3421
- [83] A. J. Bevan *et al.* [UTfit Collaboration], “The UTfit Collaboration Average of  $D$  Meson Mixing Data: Spring 2012,” JHEP **1210**, 068 (2012) doi:10.1007/JHEP10(2012)068 [arXiv:1206.6245 [hep-ph]].
- [84] J. Aebischer, J. Kumar and D. M. Straub, “Wilson: a Python package for the running and matching of Wilson coefficients above and below the electroweak scale,” arXiv:1804.05033 [hep-ph].

- [85] D. M. Straub *et al.*, “Flavio,” doi:10.5281/zenodo.594587 = <https://flav-io.github.io>.
- [86] S. Aoki *et al.*, “Review of lattice results concerning low-energy particle physics,” *Eur. Phys. J. C* **77**, no. 2, 112 (2017) doi:10.1140/epjc/s10052-016-4509-7 [arXiv:1607.00299 [hep-lat]].
- [87] A. Bazavov *et al.* [Fermilab Lattice and MILC Collaborations], “ $B_{(s)}^0$ -mixing matrix elements from lattice QCD for the Standard Model and beyond,” *Phys. Rev. D* **93**, no. 11, 113016 (2016) doi:10.1103/PhysRevD.93.113016 [arXiv:1602.03560 [hep-lat]].
- [88] L. Di Luzio, M. Kirk and A. Lenz, “Updated  $B_s$ -mixing constraints on new physics models for  $b \rightarrow s\ell^+\ell^-$  anomalies,” *Phys. Rev. D* **97**, no. 9, 095035 (2018) doi:10.1103/PhysRevD.97.095035 [arXiv:1712.06572 [hep-ph]].
- [89] For example, see J. Charles *et al.* [CKMfitter Group], “CP violation and the CKM matrix: Assessing the impact of the asymmetric  $B$  factories,” *Eur. Phys. J. C* **41**, no. 1, 1 (2005) doi:10.1140/epjc/s2005-02169-1 [hep-ph/0406184]. Updated results and plots available at: <http://ckmfitter.in2p3.fr>
- [90] For  $\mathcal{B}(B^+ \rightarrow K^+\mu^\pm\tau^\mp)$  and  $\mathcal{B}(\tau \rightarrow \mu\phi)$ , the reach numbers are taken from the talk by S. Cunliffe (on behalf of the Belle II Collaboration), 6<sup>th</sup> Workshop on Rare Semileptonic  $B$  Decays ( $b \rightarrow s\ell\ell$  2018), Munich, February 2018. For  $\mathcal{B}(\Upsilon \rightarrow \mu^\pm\tau^\mp)$ , we simply scaled up from the present upper bound.
- [91] M. Tanaka and R. Watanabe, “New physics contributions in  $B \rightarrow \pi\tau\bar{\nu}$  and  $B \rightarrow \tau\bar{\nu}$ ,” *PTEP* **2017**, no. 1, 013B05 (2017) doi:10.1093/ptep/ptw175 [arXiv:1608.05207 [hep-ph]].
- [92] B. Capdevila, A. Crivellin, S. Descotes-Genon, L. Hofer and J. Matias, “Searching for New Physics with  $b \rightarrow s\tau^+\tau^-$  processes,” *Phys. Rev. Lett.* **120**, no. 18, 181802 (2018) doi:10.1103/PhysRevLett.120.181802 [arXiv:1712.01919 [hep-ph]].
- [93] S. L. Glashow, D. Guadagnoli and K. Lane, “Lepton Flavor Violation in  $B$  Decays?,” *Phys. Rev. Lett.* **114**, 091801 (2015) doi:10.1103/PhysRevLett.114.091801 [arXiv:1411.0565 [hep-ph]].
- [94] R. S. Chivukula and H. Georgi, “Composite Technicolor Standard Model,” *Phys. Lett. B* **188**, 99 (1987). doi:10.1016/0370-2693(87)90713-1
- [95] G. D’Ambrosio, G. F. Giudice, G. Isidori and A. Strumia, “Minimal flavor violation: An Effective field theory approach,” *Nucl. Phys. B* **645**, 155 (2002) doi:10.1016/S0550-3213(02)00836-2 [hep-ph/0207036].
- [96] V. Cirigliano, B. Grinstein, G. Isidori and M. B. Wise, “Minimal flavor violation in the lepton sector,” *Nucl. Phys. B* **728**, 121 (2005) doi:10.1016/j.nuclphysb.2005.08.037 [hep-ph/0507001].
- [97] S. Davidson and F. Palorini, “Various definitions of Minimal Flavour Violation for Leptons,” *Phys. Lett. B* **642**, 72 (2006) doi:10.1016/j.physletb.2006.09.016 [hep-ph/0607329].
- [98] R. Alonso, G. Isidori, L. Merlo, L. A. Munoz and E. Nardi, “Minimal flavour violation extensions of the seesaw,” *JHEP* **1106**, 037 (2011) doi:10.1007/JHEP06(2011)037 [arXiv:1103.5461 [hep-ph]].
- [99] M. Aaboud *et al.* [ATLAS Collaboration], “Search for high-mass new phenomena in the dilepton final state using proton-proton collisions at  $\sqrt{s} = 13$  TeV with the ATLAS detector,” *Phys. Lett. B* **761**, 372 (2016) doi:10.1016/j.physletb.2016.08.055 [arXiv:1607.03669 [hep-ex]].
- [100] CMS Collaboration [CMS Collaboration], CMS-PAS-EXO-16-031.
- [101] J. M. Cline, J. M. Cornell, D. London and R. Watanabe, “Hidden sector explanation of  $B$ -decay and cosmic ray anomalies,” *Phys. Rev. D* **95**, no. 9, 095015 (2017) doi:10.1103/PhysRevD.95.095015 [arXiv:1702.00395 [hep-ph]].